

# Molecular characterization of organic aerosols in urban and forested areas of Paris using high resolution mass spectrometry

Diana L. Pereira<sup>1</sup>, Chiara Giorio<sup>2</sup>, Aline Gratien<sup>1</sup>, Alexander Zhrebker<sup>2</sup>, Gael Noyalet<sup>1</sup>, Servanne Chevaillier<sup>3</sup>, Stéphanie Alage<sup>3</sup>, Elie Almarj<sup>1</sup>, Antonin Bergé<sup>1,a</sup>, Thomas Bertin<sup>3</sup>, Mathieu Cazaunau<sup>3</sup>, Patrice Coll<sup>1</sup>, Ludovico Di Antonio<sup>3</sup>, Sergio Harb<sup>3,7</sup>, Johannes Heuser<sup>3</sup>, Cécile Gaimoz<sup>3</sup>, Oscar Guillemant<sup>3,4</sup>, Brigitte Language<sup>3,b</sup>, Olivier Lauret<sup>3</sup>, Camilo Macias<sup>1</sup>, Franck Maisonneuve<sup>3</sup>, Bénédicte Picquet-Varrault<sup>3</sup>, Raquel Torres<sup>3,c</sup>, Sylvain Triquet<sup>1</sup>, Pascal Zapf<sup>3</sup>, Lelia Hawkins<sup>5</sup>, Drew Pronovost<sup>5</sup>, Sydney Riley<sup>5</sup>, Pierre-Marie Flaud<sup>6</sup>, Emilie Perraudin<sup>6</sup>, Pauline Pouyes<sup>6</sup>, Eric Villenave<sup>6</sup>, Alexandre Albinet<sup>7</sup>, Olivier Favez<sup>7</sup>, Robin Aujay-Plouzeau<sup>7</sup>, Vincent Michoud<sup>1</sup>, Christopher Cantrell<sup>3</sup>, Manuela Cirtog<sup>3</sup>, Claudia Di Biagio<sup>1</sup>, Jean-François Doussin<sup>3</sup> and Paola Formenti<sup>1</sup>

<sup>1</sup>Université Paris Cité et Univ Paris Est Creteil, CNRS, LISA, Paris, F-75013, France

<sup>2</sup>Yusuf Hamied Department of Chemistry, University of Cambridge, Cambridge, CB2 1EW, United Kingdom

<sup>3</sup>Université Paris Est Creteil and Université Paris Cité, CNRS, LISA, Créteil, F-94010, France

<sup>4</sup>Université Paris-Saclay, Ecole Normale Supérieure Paris-Saclay, 4 avenue des sciences, 91190 Gif-sur-Yvette, France

<sup>5</sup>Department of Chemistry, Harvey Mudd College, 301 Platt Blvd, Claremont, California 91711, United States

<sup>6</sup>Univ. Bordeaux, CNRS, EPOC, EPHE, UMR 5805, F-33600 Pessac, France

<sup>7</sup>INERIS, Parc technologique Alata BP2, 60550 Verneuil en Halatte, France

<sup>a</sup>now at Laboratoire des Sciences du Climat et de l'Environnement, CEA-CNRS-UVSQ, IPSL, Université Paris–Saclay, 91191 Gif-sur-Yvette, France

<sup>b</sup>now at Unit for Environmental Sciences and Management, North-West University, Potchefstroom, South Africa

<sup>c</sup>now at Center for Research in Sustainable Chemistry-CIQSO, University of Huelva, Campus de El Carmen, E-21071, Huelva, Spain

Correspondence to: [diana.pereira@lisa.ipsl.fr](mailto:diana.pereira@lisa.ipsl.fr), [aline.gratien@lisa.ipsl.fr](mailto:aline.gratien@lisa.ipsl.fr)

**Abstract.** In order to study aerosols in environment influenced by anthropogenic and biogenic emissions to variable extents, PM<sub>1</sub> samples were collected during the summer 2022 in the greater Paris area (ACROSS campaign, Atmospheric Chemistry Of the Suburban Forest, June 14 to July 25) at two locations that represent the urban Paris and the suburban forested area. They were analyzed using high resolution mass spectrometry (HRMS) together with total carbon (TC) by a thermo-optical method. Both sites are compared here to explore differences in aerosol composition from urban and forested environments. The TC analysis shows similar organic carbon (OC) concentrations at both sites ( $3.2 \pm 1.8 \mu\text{g m}^{-3}$  for Paris and  $2.9 \pm 1.5 \mu\text{g m}^{-3}$  for Rambouillet), and higher elemental carbon (EC) values in the urban area. Both OC and EC concentrations did not show significant variations for daytime and nighttime conditions. This work highlights the influence of anthropogenic inputs into the chemical composition of urban and forested areas, derived into the presence of CHO and CHON compounds but also the detection of two sulfur-containing compounds ( $\text{C}_5\text{H}_{12}\text{SO}_7$  and  $\text{C}_{10}\text{H}_{17}\text{NSO}_7$ ), which could be tentatively assigned as organosulfates. A smaller number of aromatic compounds were observed for clean periods, that better represent the local biogenic and anthropogenic contributions in Rambouillet and Paris, respectively.

## 1 Introduction

Organic aerosols (OA) represent an important fraction of the fine aerosol mass (up to 90%) (Chen et al., 2022; Kanakidou et al., 2005) that can impact the Earth's climate through their interactions with clouds (Andreae and Rosenfeld, 2008; IPCC, 2023; Rosenfeld et al., 2014), solar radiation (Haywood, 2016), and air quality (Chen and Kan, 2008). Despite the importance of these particles, their composition and formation processes are not fully understood and gaps remain in their chemical characterization and description (Akinyoola et al., 2024; Kalberer, 2015). Different environments provide different aerosol sources with varied chemical composition and influence on the atmosphere. Megacities such as Paris, Mexico City, Beijing, and New York are known for their high populations and local anthropogenic emissions that contribute to the atmospheric particulate matter (PM) levels (Karagulian et al., 2015; Cheng et al., 2016), while remote environments such as forested areas and oceans, contribute mostly with biogenic emissions (Shen et al., 2015; Zhu et al., 2016). At their interfaces, urban and remote environments can be affected by mixtures of both biogenic and anthropogenic emissions which influence OA formation and composition (RattanaVaraha et al., 2016; McFiggans et al., 2019; Shrivastava et al., 2019). The enhancement of biogenic aerosol formation under the influence of anthropogenic pollutants has already been reported (Bryant et al., 2023; RattanaVaraha et al., 2016; Shrivastava et al., 2019; Yee et al., 2020); however, the opposite effect for specific mixtures such as isoprene, CO or CH<sub>4</sub> with  $\alpha$ -pinene was also observed (McFiggans et al., 2019), highlighting the complexity of OA formation in mixed environments.

Complex and simultaneous physicochemical processes influence aerosol formation and growth (Hallquist et al., 2009) in the atmosphere. Therefore, intensive and long-term field observations using combinations of online and offline techniques have been performed to gain insights into OA chemical composition, source apportionment, properties and possible implications on the atmospheric processes (Molina et al., 2010; Bressi et al., 2013; Zhang et al., 2013; Artaxo et al., 2017; Cantrell and Michoud, 2022). These techniques include online aerosol mass spectrometers (Zhang et al., 2007), total carbon content with semi-continuous carbon analyzers (Karanasiou et al., 2020) or offline thermo-optical techniques (Cao et al., 2005; Ma et al., 2016), and chemical composition of samples collected on filters (Yan et al., 2009; Ding et al., 2012; Michoud et al., 2021) particularly using chromatographic techniques coupled to mass spectrometers (Kourtchev et al., 2013). High resolution mass spectrometers (e.g., Orbitrap) have been shown to provide interesting insights for OA in urban, sub-urban and/or remote areas (Kourtchev et al., 2014; Daellenbach et al., 2019; Giorio et al., 2019; Wang et al., 2022; Amarandei et al., 2023). For example, a strong biogenic influence at a urban background and two remote locations in the Alpine Valleys in Switzerland was observed during summertime (Daellenbach et al., 2019). High contribution of saturated oxidized compounds together with the presence of organosulfates suggested that Secondary Organic Aerosol (SOA) formation from biogenic VOC precursors plays an important role during the summer even in urban areas (Giorio et al., 2019; Amarandei et al., 2023). The importance of anthropogenic oxidized compounds has also been highlighted, with a strong contribution from traffic emissions in urban areas (Kourtchev et al., 2014; Wang et al., 2022).

The Paris area (comprising Paris city and its suburbs) is a relatively compact urban zone of ca. 40 km by 40 km surrounded by low urbanized areas mostly composed of intensive agriculture fields and forest. Mixing between anthropogenic and biogenic emissions can occur, especially when the plume of Paris travels away from the city. This encounter can be favour by anticyclonic weather that allows the interaction between air masses due to slow moving conditions (Lagmiri & Dahech, 2023; Wei et al., 2011). Anticyclone conditions has previously led to the identification of PM accumulation (Beekmann et al., 2015) and variability of aerosol particles (Bressi et al., 2013) at the Paris region. In consequence, mixing between anthropogenic and biogenic emissions can occur especially when the plume of Paris travels away from the city at low velocity and altitude which is often the case under anticyclonic conditions (Lagmiri and Dahech, 2023). Previous studies in this area involving offline analysis of the aerosol chemical composition have been focused on total carbon (TC) determination (Favez et al., 2009), combined with ion chromatography analysis (Hodzic et al., 2006; Gros et al., 2007; Sciare et al., 2010; Bressi et al., 2013) and only a few reported analysis at the molecular scale (Lanzafame et al., 2021; Srivastava et al., 2018, 2019). Gros et al. (2007) reported the traffic pollution as an important aerosol source in the Paris urban area as seen from the measurement site located at the Paris City Hall during the spring period. Analyses performed during the summer at the suburban area of Saclay (25 km southwest from Paris) showed the predominance of primary aerosols and highlighted the contribution of both anthropogenic and biogenic sources (Hodzic et al., 2006). Previous measurements in central Paris showed the influence of residential wood burning emissions in the winter (Favez et al., 2009) and highlighted the local contributions for the primary fraction of the aerosol and continental photochemical-aged air masses during the spring (Sciare et al., 2010).

All of these studies were mostly based on a single sampling point, with the exception of Bressi et al., (2013) who compared the chemical composition of a set of samples collected at five sites of the AIRPARIF air quality stations during one-year measurements (September, 2009 to September, 2010). Those sites included one urban location at the Paris center (4<sup>th</sup> district), one suburban station (10 km northeast from Paris center station), and three rural sites located at 65 km northeast, 50 km northwest and 60 km south from the urban station. Based on ions analysis and TC measurements only, a spatial homogeneity of the aerosol chemical composition was observed during that period for the sites, with higher levels of local anthropogenic contributions as the sites get closer to the Paris center. Those studies provided a base for the typology of aerosol sources with a limited ion spectrum ( $\text{NO}_3^-$ ,  $\text{SO}_4^{2-}$ ,  $\text{Na}^+$ ,  $\text{NH}_4^+$ ,  $\text{K}^+$ ,  $\text{Mg}^{2+}$ , and  $\text{Ca}^{2+}$ ) analyzed. This together with similarities between sites observed for long measurement periods and the lack of seasonal tendencies, arises the concern that description of the inorganic aerosol fraction and OC measurements cannot properly capture the full chemical process occurring. Recent studies focus on measurements of the OA at the suburban SIRTa (Site Instrumental de Recherche par Télédétection Atmosphérique, Haefelin et al., 2005) site (Lanzafame et al., 2021; Srivastava et al., 2018, 2019), located at the southwest of the Paris center (25 km). Influence of secondary processes in the aerosol composition from the early spring was observed by Srivastava et al. (2018, 2019). The temporal variability of pinene, isoprene,  $\beta$ -caryophyllene, anthropogenic SOA acids and nitroaromatic markers was investigated, showing a seasonal dependence of the processes enlighten by nitroaromatic and isoprene markers (Lanzafame et al., 2021).

The aforementioned studies showed the contribution of different local urban sources mainly associated to traffic emissions, especially during the summer, together with contributions of mid- and long-range transported biogenic and anthropogenic species, from primary or secondary origin. They additionally highlighted the effect of the seasonal variability for different specific species associated with emission factors and seasonal meteorological conditions. The studies performed to understand the atmospheric chemical composition of rural, suburban, and urban areas in Paris provide important information on the major chemical fractions, carbon content, and some molecular tracers, however information on the OA chemical composition and its temporal and spatial variability is still missing. Building upon the existing knowledge, our work aims at providing new description of the molecular composition and day/night variability of the OA fraction from simultaneous measurements in two urban and forested environments in the Paris region in summer 2022 from measurements performed in the framework of the ACROSS (Atmospheric Chemistry Of the Suburban Forest) intensive campaign.

## 2 Methods

Atmospheric measurements were performed during the ACROSS campaign, which aims to understand the mixing between the biogenic and anthropogenic emissions and their impact into aerosol formation and aging. In the Paris urban area anthropogenic compounds can be emitted and exported to the urban areas, interacting with their local emissions. Therefore, during ACROSS, measurements were performed at ground-based, airborne, and space-based platforms located at different urban, semi-urban and rural locations in the greater Paris area. Further details of the sites and campaign description are provided in Cantrell & Michoud (2022). In this work, we focus on the aerosol chemical composition measurements performed at ground level at two locations that represent the urban Paris and the suburban forested area.

### 2.1 Ground level sampling

Atmospheric sampling was performed in summer 2022 (June 14 – July 25) ~~during the ACROSS campaign (Cantrell and Michoud, 2022)~~ at the 7<sup>th</sup> floor terrace of the Lamarck B building at the Université Paris Cité, located at 20 m above ground level (m.a.g.l) (48.8277 °N and 2.3806 °E, named as Paris herein) and at ground level in the Rambouillet forest (48.6866 °N and 1.7045 °E, named as Rambouillet herein).





**Figure 1: Sampling sites in the Paris region for aerosol sampling in the ACROSS campaign during summer 2022. Map in the left shows the spatial disposition between sites (MathWorks Inc, 2022). The urban area sampling site is located at the Université Paris Cité and the forested one is at the Rambouillet forest, displayed on the right side (©Google Earth).**

Paris city with a population of ~2 million inhabitants (Bilan démographique, 2024) and about 12 million in whole Paris greater area, is characterized by urban local emissions from traffic and aerosol contributions from mid- and long-range transport (Beekmann et al., 2015; Bressi et al., 2013, 2014). On the contrary as observed in Fig.1, Rambouillet Site is a dense forest area located 43 km from the centre south-west bound of Paris, far from local anthropogenic contributions and susceptible to the influence to urban plumes arrival from the north east. Rambouillet forest is mainly consisting of oaks and pine trees (Office National des Forêts, 2023) and has an extension of 14 000 ha.

### 2.1.1 Filter sampling

Aerosol filter sampling of the  $PM_{10}$  fraction was performed during day (6:00 – 22:00, local time) and night (22:00 – 6:00, local time) on 150 mm diameter quartz fiber filters (Pallflex Tissuquartz). Samples were collected, using an automatic continuous high-volume aerosol sampler (30 m<sup>3</sup> h<sup>-1</sup>) DHA-80 (DIGITEL Enviro-Sense) equipped with a  $PM_{10}$  sampling head, directly exposed to the ambient air. Sampling times were selected to account for different daily process in the presence of sunlight (day-time) and in the absence of light (night-time). Therefore, sampling performed during day will include an important fraction of anthropogenic activities mainly associated to traffic contribution at rush hours between 8:00-10:00 and 20:00-22:00 as previously reported in the Paris urban area (Gros et al., 2007; Sciare et al., 2010). Prior sampling, the quartz fiber filters were conditioned at 550 °C for 8 hours and conserved in pre-baked aluminum foil, sealed in plastic bags. After exposure, samples were conserved in pre-baked and sealed aluminum foils at -20 °C, then transported to the laboratory, where they were punched to smaller fractions ( $\varnothing = 30$  mm and 46 mm) for chemical analysis. The smaller fractions were also conserved following the same protocol.

### 2.1.2 Additional data

Meteorological parameters such as relative humidity (RH), temperature, and wind speed and direction for the Rambouillet site were provided by the Centre National de Recherches Météorologiques (CNRM) through the MeteoFrance mobile facility (Denjean, 2023). Additional data of NO<sub>x</sub>, O<sub>3</sub> and SO<sub>2</sub> concentrations for Rambouillet were collected by monitors from the Portable Gas and Aerosol Sampling UnitS (PEGASUS) mobile facility (Giorio et al., 2022). At PEGASUS, gas measurements were performed using Teflon tubes with 6.35 diameter with the lines inlet placed at the top of the container at 2 m.a.g.l. A NO<sub>x</sub> Monitor APNA370 (Horiba) based on O<sub>3</sub> chemiluminescence, an O<sub>3</sub> Monitor APOA370 (Horiba) based on UV absorption and a SO<sub>2</sub> Monitor Horiba APSA370 based on UV fluorescence. At the Paris site, we used a meteorological station Lufft WS600 (Di Antonio et al., 2023), a NO<sub>x</sub> monitor AC32M (Environment SA) based on O<sub>3</sub> chemiluminescence, an O<sub>3</sub> monitor 41M (Environment SA) based on UV absorption and a SO<sub>2</sub> Monitor AF22 (Environment SA) based on UV fluorescence. For Paris, gas sampling was performed at the top of the building (30 m a.g.l) through a 12 m long Teflon tube, with a 17.5 mm inner diameter at 40 L min<sup>-1</sup>, until a glass manifold where all gas phase instruments sampled ambient air.

### 2.2 Chemical analysis

Organic carbon (OC) and elemental carbon (EC) were measured using a thermo-optical analyzer (Sunset Laboratory Inc.) on a 1.5 cm<sup>2</sup> filter surface following the EUSAAR2 protocol (Cavalli et al., 2010). The Sunset analyzer was calibrated using a sucrose (purity > 99.5 %) solution on a 1.5 cm<sup>2</sup> filter surface at concentrations between 0.42 µgC cm<sup>-2</sup> and 40 µgC cm<sup>-2</sup>, with a limit of detection of 0.25 µgC cm<sup>-2</sup> and a limit of quantification of 0.42 µgC cm<sup>-2</sup>. Prior to each analysis, an instrumental blank and a point at 10 µgC cm<sup>-2</sup> were measured as a quality control. OC and EC values were automatically calculated with the software OCBC835 (Sunset Laboratory) and the split point was manually verified to ensure proper assignation. Uncertainties on the measurements were obtained by considering the 5% of the carbon concentration plus 0.1 µgC cm<sup>-2</sup> as minimum instrumental error as suggested by the manufactured (Sunset Laboratory).

The chemical compositions of OA extracts were studied using high resolution mass spectrometry (HRMS). Filters of 46 mm diameter were placed in pre-cleaned glass vials and extracted three times in 3 mL methanol (LC-MS grade, Fisher Scientific) by 30 min sonication in slurry ice. Filters of 46 mm diameter were extracted three times by 30 min sonication in slurry ice with 3 mL of methanol (LC-MS grade, Fisher Scientific) in pre-cleaned glass vials. Methanol was used due to its suitability for the extraction of polar unsaturated compounds (Zherebker et al., 2024) and high extraction efficiency of OA (Giorio et al., 2019) enabling analysis without extra purification step. Extracts were combined for each sample and filtered with 0.45 µm and 0.2 µm syringe filters (Iso-Disc™ Filters PTFE, Ø 4 mm) consecutively. The solvent was partially evaporated using a gentle stream of nitrogen to 400 µL. The final solutions were stored at -18°C prior to analysis. Additional details of the extraction protocol can be found in Kourtchev et al. (2014).

Non-target mass spectrometric analysis was performed using LTQ Orbitrap mass spectrometer (Thermo Scientific) equipped with a chip-based nanoESI source (TriVersa NanoMate, Advion) operating in negative ionization mode. The source parameters

were: gas pressure of 0.30 psi, spray voltage -1.4 kV, and an injection volume of 7  $\mu$ L. NanoESI source was used to achieve higher ionization efficiency for a variety of analytes (Kourtchev et al., 2014). All spectra were recorded in triplicates with one-minute data acquisition time, with a nominal resolution of 100,000, and in two scan ranges (50-500 m/z and 150-1000 m/z).

Due to the solvent selection and the use of the ESI source, analysis at molecular scale focus on the polar fraction of the methanol soluble OA.

### 2.3 HRMS data processing

HRMS data treatment was conducted following Zielinski et al. (2018). Peaks were extracted and assigned using Xcalibur 2.1 (Thermo Scientific) with a mass tolerance of 4 ppm. Atomic constraints for formulae assignment were:  $^{14}\text{N}$  (0-5),  $^{16}\text{O}$  (0-50),  $^{12}\text{C}$  (1-100),  $^1\text{H}$  (1-200),  $^{32}\text{S}$  (0-2),  $^{34}\text{S}$  (0-1), and  $^{13}\text{C}$  (0-1). Formula lists and peak intensities were further processed including internal calibration, noise removal, blank subtraction, and additional atomic constraints: elemental ratios were set as  $0.3 \leq \text{H/C} \leq 2.5$ ,  $\text{O/C} \leq 2$ ,  $\text{N/C} \leq 1.3$ ,  $\text{S/C} \leq 0.2$ ,  $^{13}\text{C}/^{12}\text{C} \leq 0.011$  and  $^{34}\text{S}/^{32}\text{S} \leq 0.045$ , double bond equivalent (DBE) values, nitrogen rule, and isotopic filtering (Zielinski et al., 2018). Formulae with smallest absolute mass errors were used for multiple assignments after mass shift correction, and only formulae found in all triplicates were considered. ~~Five families of compounds were defined based on their molecular composition: CHO, CHON, CHOS, CHONS, and CHNS. CHN and CHS families were not considered here as they cannot ionize in the negative mode. The formulae assigned were grouped based on the molecular composition as CHO, CHON, CHOS, CHONS, CHNS, CHN and CHS families. However, due to the higher ionization efficiency in the negative mode, this work focus on O-containing compounds (CHO, CHON, CHONS and CHOS). This selection is also supported by the predominance of oxygenated compounds on the OA on the PM<sub>1</sub> fraction reported at different urban and rural areas (Zhang et al., 2007).~~

After formula assignment, van Krevelen (VK) diagrams (Kim et al., 2003) were used to visualize the differences between the samples from Paris and Rambouillet. Following Kourtchev et al. (2013), three compound domains such as aliphatic, low oxygenated aromatic and more oxidized aerosol were used herein. The aliphatic group was attributed at low O/C ratios ( $< 0.5$ ) and high H/C ( $> 1.5$ ), low oxygenated aromatic domain was present at  $\text{O/C} < 0.5$  and  $\text{H/C} > 0.5$ , and more oxidized compounds could be found at higher O/C ( $> 0.5$ ). More details are presented in the Supplementary material.

The aromaticity equivalent ( $X_c$ ) of the aerosol samples of Rambouillet and Paris were calculated following Yassine et al. (2014) through Eq. 1:

$$X_c = \frac{3[\text{DBE} - (m\text{O} + n\text{S})] - 2}{\text{DBE} - (m\text{O} + n\text{S})} \quad (1)$$

The  $m, n$  parameters designates the fractions of O and S atoms involved in the  $\pi$ -bonds. In order to provide a conservative estimate for unsaturation accounted for only carbon-carbon  $\pi$ -bonds, we used  $m, n = 0.5$ , which correspond to the maximum possible fraction of  $\text{sp}^2$ -hybridized oxygen atoms as carboxyl groups. While conservative approach provides only a lower boundary for the contribution of highly unsaturated compounds (tentatively assigned as aromatic and condensed compounds).

a predominance of carboxylic acid species over other functionalities is expected for analysis in negative ion mode (Kourtchev et al., 2016). The role of carboxylic acids as one of the major fractions of aerosol particles was observed during the summer for field samples at European cities at Corsica (Michoud et al., 2021) and Czech Republic (Horník et al., 2020). Although this assumption can lead to an underestimation of possible aromatic fraction, we considered the  $m,n=0.5$  as previously applied in the literature (Tong et al., 2016; Yassine et al., 2014). The constants  $m,n=0.5$  are the fractions of heteroatoms involved in the  $\pi$  bond structure for oxygen and sulfur, assuming that the signals identified here belong to carboxylic acids ( $R-COOH$ ), as measurements are performed in the negative ionization mode (Kourtchev et al., 2016). DBE represents the degree of unsaturation of a compound (Wozniak et al., 2008) and it is computed considering the number of C, H, and N atoms as follows:

$$DBE = 1 + \frac{1}{2}(2C - H + N) \quad (2)$$

Yassine et al. (2014) proposed threshold values of  $X_c$ , where  $X_c \geq 2.5$  account for aromatics and  $X_c \geq 2.71$  for condensed aromatics. Following this classification, the  $X_c$  are calculated and grouped here as unsaturated ( $X_c < 2.5$ ), aromatic ( $2.5 \leq X_c < 2.71$ ) and condensed aromatic ( $X_c \geq 2.71$ ) compounds. Aromatics may contain one benzene ring, while condensed aromatics can contain fused rings.

## 2.4 Statistical analysis

Pearson correlation and pairwise cosine distances were calculated to analyze the existing relationships between chemical composition (OC and EC concentrations, number of formulae), meteorological conditions and anthropogenic contaminants observed during the campaign. Atmospheric conditions used for correlation analysis are reported in Table S1 and they represent average data observed during the sampling period.

## 3 Results and discussion

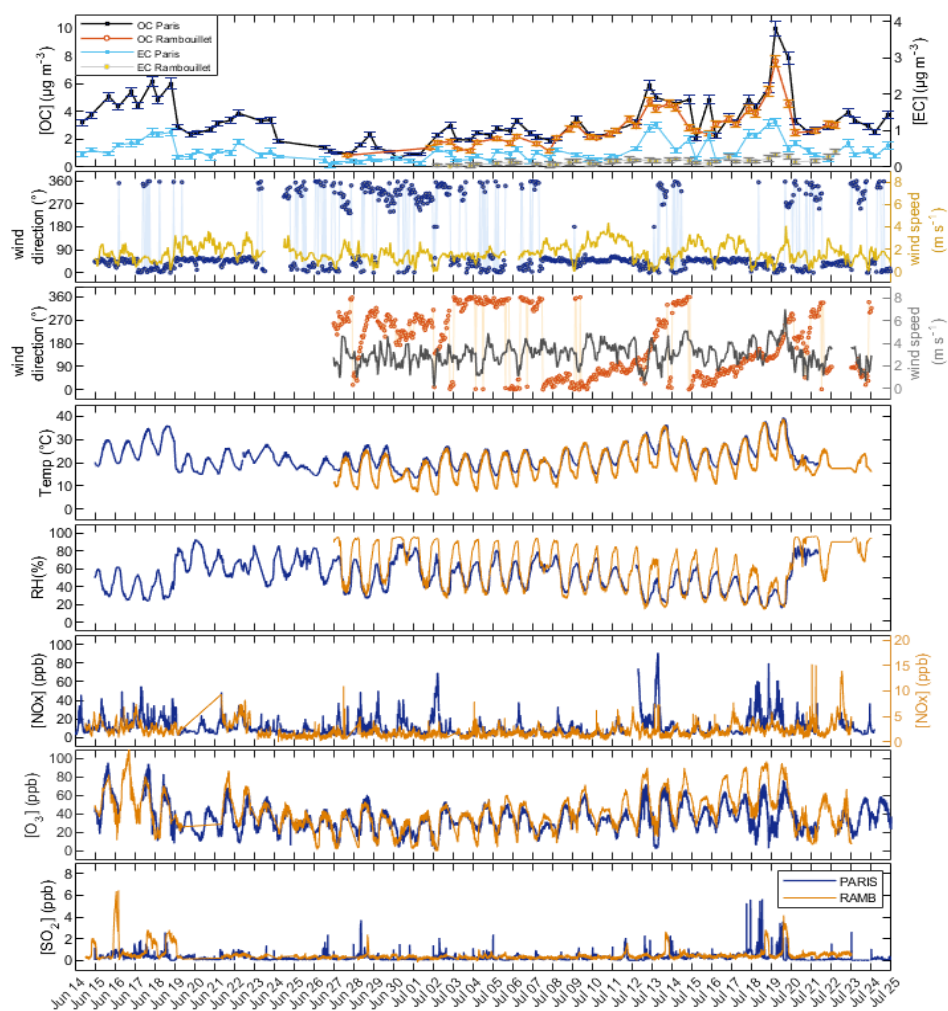
### 3.1 Variability of OC and EC concentrations

The OC and EC concentrations observed during the summer 2022 at Paris and Rambouillet are summarized in Fig. 2. In Paris, OC concentrations ranging from 0.7 to 10.0  $\mu\text{g m}^{-3}$  and maximum EC concentrations of 1.3  $\mu\text{g m}^{-3}$  were observed between June 14 and July 25. A shorter dataset is available for Rambouillet, between June 27 to July 22, with OC concentrations varying between 0.8 and 7.7  $\mu\text{g m}^{-3}$ . The OC time series of Paris showed higher concentrations at the beginning of the campaign (June 14 and June 24) and after July 12, while for Rambouillet there was an increasing trend over time which coincides temporally with the increased OC concentration observed from the end of June to July for Paris. Wind direction showed a north to east ( $0^\circ$  to  $75^\circ$ ) predominant contribution at the beginning of the period (before June 24) and additional contributions from west ( $230^\circ$  to  $355^\circ$ ) air masses for Paris. In Rambouillet, a similar behavior was observed at the beginning of July while a transition

from north-east to west was observed for the rest of the period. Wind directions from north-east (between 0° and 90°) suggests the possible impact of Paris emissions into the forest during the second week of July from 7 to 13 and 15 to 16. Higher wind speed values were observed over the forest site (up to 7.1 m s<sup>-2</sup>) than for downtown Paris (up to 4.3 m s<sup>-2</sup>).

The temporal variability of RH, temperature and concentrations of NO<sub>x</sub>, O<sub>3</sub> and SO<sub>2</sub> at both sites is also shown in Fig. 2. Mean values of RH of 51.7 % (min 16.0 % and max 93.0 %) and temperature of 22.5 °C (min 13.3 °C and max 39.5 °C) were observed for the Paris site. In Rambouillet, mean values of 60.6 % (min 14.4 % and max 96.7 %) and 19.8 °C (min 6.0 °C and max 38.9 °C) were reported for RH and temperature, respectively. Higher values of NO<sub>x</sub> were observed in Paris (mean values of 10.7 ppb and 2.2 ppb with maximum concentrations of 90.9 ppb and 15.2 ppb for Paris and Rambouillet respectively) while O<sub>3</sub> concentrations followed a similar profile at both sites with higher concentrations in Rambouillet of 6.0 ppb on average. Low SO<sub>2</sub> concentrations were observed for both sites with values being generally below 1ppb but some peaks were also detected with maximum values of 8.5 and 6.5 ppb for Paris and Rambouillet, respectively. Averages over the filter sampling times for the parameters described are presented in Table S1.

The difference between the forested and urban environment is observed at looking into the EC concentrations, which are higher in Paris due to the densely populated area, which translates into higher local anthropogenic activities. In contrast, similarities between the profiles of the OC concentrations for the common period between both sites (June 27 to July 22) may suggest common organic sources influencing the chemical composition. Given that different wind directions are observed after July 8, these similarities can be influenced by local sources and transported air masses. Previous summer measurements (Gros et al., 2007) of OC in the Paris urban area highlight local traffic contributions. As observed at both sites, the increasing of the OC concentrations at the end of July was accompanied by an increase of temperature, NO<sub>x</sub> and O<sub>3</sub>, which can enhance the chemistry and derive into a higher OA formation (Luo et al., 2021; Shrivastava et al., 2019; Xu et al., 2022). Further influence of the meteorological parameters and anthropogenic pollutants into the OC concentrations and composition are explored in Section 3.3.



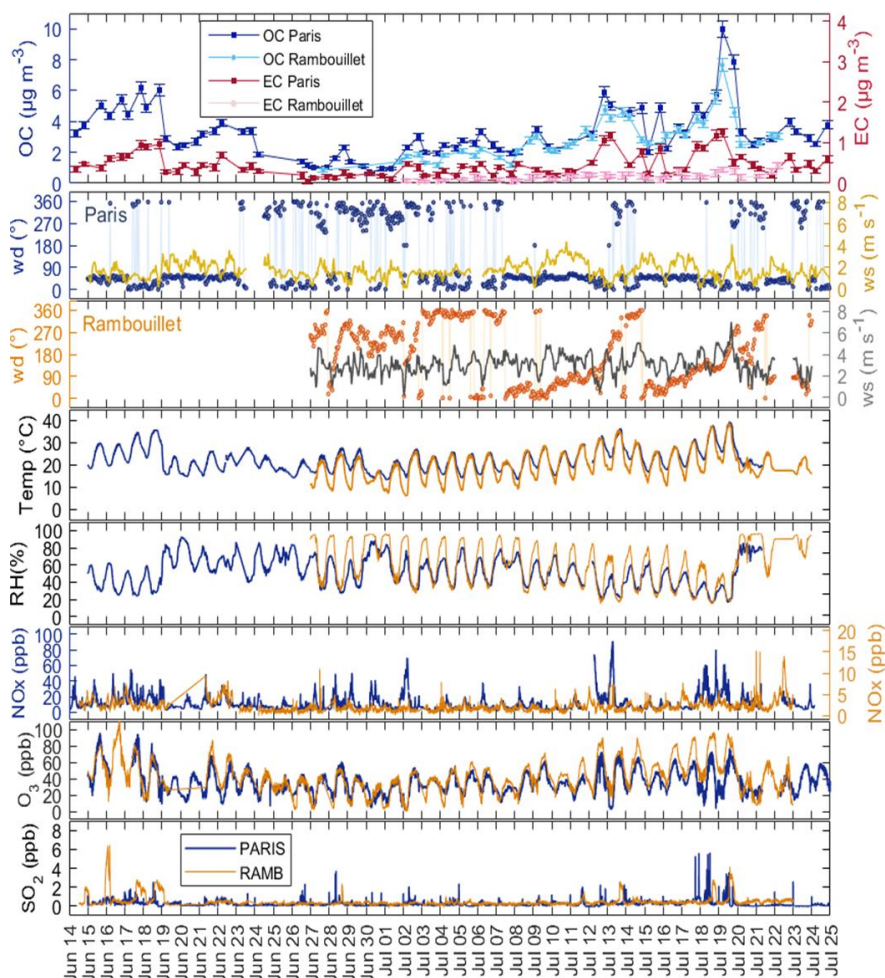


Figure 2: Temporal series of the OC, EC, NO<sub>x</sub>, O<sub>3</sub> and SO<sub>2</sub> concentrations and wind conditions observed during the summer 2022 between June 14 and July 25. Data for OC and EC for Paris (blue) and Rambouillet (orange and gray) are reported with their standard deviations represented by the error bars, accounting for sample density variations and instrumental errors. Wind conditions are presented by wind speed (yellow and gray) and wind direction (blue and orange), and reported here for hourly average of daily measurements. Measurements for NO<sub>x</sub>, O<sub>3</sub> and SO<sub>2</sub> for Paris (blue) and Rambouillet (orange) were performed at 30 m a.g.l. in Paris and at ground level in Rambouillet.

Mis en forme : Centré

In this study, mean OC concentrations of  $3.2 \pm 1.78 \mu\text{g m}^{-3}$  and  $2.9 \pm 1.5 \mu\text{g m}^{-3}$  were observed for [the whole sampling period at Paris and Rambouillet](#), respectively. Such values are around the annual local/regional averages previously found in  $\text{PM}_{2.5}$  by Bressi et al., (2013), who reported  $3.0 \mu\text{g m}^{-3}$  in the urban center of Paris,  $3.2 \mu\text{g m}^{-3}$  at a suburban site (10 km from Paris center), and between 2.1 and  $2.9 \mu\text{g m}^{-3}$  in the rural areas at the north and south of Paris, located >50 km from the center. Concentrations in the present analysis, are also in line with the average summertime OC concentration of  $2.9 \mu\text{g m}^{-3}$  at the suburban (southwest of Paris center) SIRTa site reported by Lanzafame et al., (2021).

Mean OC [and EC](#) concentrations for Rambouillet observed in this study fall in a similar range than mean values of  $3.6 \mu\text{g m}^{-3}$  and  $0.1 \mu\text{g m}^{-3}$  reported in the rural area of Hyttiala (Finland) for the  $\text{PM}_1$  fraction (Daellenbach et al., 2019) and  $4.2 \mu\text{g m}^{-3}$  and  $0.2 \mu\text{g m}^{-3}$  for the  $\text{PM}_{2.5}$  in the forest on the Great Hungarian Plain (Hungary) (Ion et al., 2005; Kourtchev et al., 2009). Our average OC [and EC](#) concentrations in Paris are of the same order of magnitude than those measured in the urban area of Seoul (Korea), where OC and EC concentrations of  $3.5 \mu\text{g m}^{-3}$  and  $1.6 \mu\text{g m}^{-3}$  for  $\text{PM}_{2.5}$  were reported (Yoo et al., 2022). While our mean OC concentration at Paris is of the same magnitude, the EC concentration in Seoul is 4 times higher (Yoo et al., 2022) than the observed in this study ( $0.4 \mu\text{g m}^{-3}$ ).

### 3.1.1 Diurnal variations of OC and EC concentrations

For the periods of data overlap for the two sampling sites (June 27 to July 22), Fig. 2 shows a similar trend for the OC concentrations for most of the days with close mean concentrations values for OC of  $3.42 \pm 1.8 \mu\text{g m}^{-3}$  in Paris and  $2.9 \pm 1.5 \mu\text{g m}^{-3}$  in Rambouillet ([Table 1](#)[Table 4](#)) and good OC concentrations correlations between both sites ( $r > 0.70$ ,  $p\text{-value} < 0.05$ ) as shown in Fig. S1. [Additionally, at correlating OC concentrations during day time at Paris and night time at Rambouillet, the moderate positive correlation value of 0.55 \(p-value=0.02\) suggest that some organic compounds could be form in the urban area, transported to the forested one and influence the chemical composition of the consecutive filter.](#)

**Table 1. Summary of OC and EC concentrations observed at Paris and Rambouillet during the summer 2022. Maximum, minimum and mean concentrations are reported for the total data collected from June 14 to July 25. Day and night values of the concentrations are reported for the period of data overlap for the two sites (June 27 to July 22). The mean concentrations are reported with their standard deviation along the time series.**

	Paris		Rambouillet	
	OC ( $\mu\text{g m}^{-3}$ )	EC ( $\mu\text{g m}^{-3}$ )	OC ( $\mu\text{g m}^{-3}$ )	EC ( $\mu\text{g m}^{-3}$ )
All data – mean	$3.2 \pm 1.78$	$0.4 \pm 0.3$	$2.9 \pm 1.5$	$0.2 \pm 0.1$
(min – max)	(0.7– 10.0)	(0.1 - 1.3)	(0.8 - 7.7)	(0.0 - 0.4)
<a href="#">Overlap period – mean</a>	<a href="#">3.4 ± 1.8</a>	<a href="#">0.5 ± 0.3</a>	<a href="#">2.9 ± 1.5</a>	<a href="#">0.2 ± 0.1</a>
<a href="#">(min – max)</a>	<a href="#">(1.0– 10.0)</a>	<a href="#">(0.1 - 1.3)</a>	<a href="#">(0.8 - 7.7)</a>	<a href="#">(0.0 - 0.4)</a>
Daytime – mean	$3.1 \pm 1.8$	$0.5 \pm 0.3$	$2.8 \pm 1.5$	$0.2 \pm 0.1$
(min – max)	(1.0 – 10.0)	(0.1 - 1.3)	(0.8 - 7.7)	(0.1 – 0.4)
Nighttime – mean	$3.7 \pm 1.7$	$0.5 \pm 0.4$	$3.1 \pm 1.6$	$0.2 \pm 0.1$
(min – max)	(0.9 - 7.8)	(0.2 - 1.2)	(1.2 – 5.5)	(0.0 – 0.3)



Measured OC and EC concentrations were compared for both sites in Table 1 for day and night periods. Higher EC concentrations were observed for Paris than for Rambouillet with maximum daytime values of  $1.3 \mu\text{g m}^{-3}$  and night values of  $1.2 \mu\text{g m}^{-3}$ . Higher EC concentrations for Paris highlights the urban nature of the site, while EC detection was not expected at Rambouillet, given its forested nature. In Paris, mean OC concentrations of  $3.1$  and  $3.7 \mu\text{g m}^{-3}$  were observed during day and night, while in Rambouillet mean values of  $2.8$  and  $3.1 \mu\text{g m}^{-3}$ . Non-significant variability was observed between day and night for OC and EC concentrations. The proximity of the values for day and night concentrations observed at both sites (Table 1) and the similar trends (Fig. 2), together with the good correlations observed for OC concentrations (Fig. S1) may suggest common sources and/or air masses affecting the OA composition of both sites.

Temperature variations between day and night periods associated with the solar irradiance together with higher ozone concentrations observed at day for both sites (Fig. 2) highlights the influence of different oxidation processes influencing the OC concentrations during the day. Higher temperature observed during the day can also enhance SOA precursors emissions such as monoterpenes (Bourtsoukidis et al., 2024; Malik et al., 2023), which then influence photochemical OA formation (Lin et al., 2009). At night, lower temperatures may favor the transition to the particle phase (Cahill et al., 2006; Giorio et al., 2019) and nitrate radical chemistry can affect SOA formation (He et al., 2021), increasing the OC concentrations. In addition to the influence of temperature, the planetary boundary layer (PBL) dynamics can influence OC and EC concentrations. During the day, the boundary layer height is deeper due to solar heating, which influence the mixing and dilution of pollutants. While during the night, the PBL becomes shallow causing a nocturnal stability, which can enhance pollutants concentrations (Li et al., 2021; Wang et al., 2023; Zhang et al., 2020). Therefore, the lack of tendencies for OC and EC concentrations between day and night can results from a combination of different atmospheric processes.

Specific samples were selected to further understand differences in the aerosol chemical composition using the OC concentration and pollutants concentrations as indicators of chemistry. Samples from July 3 and 4 showed OC concentrations below the average (i.e.,  $3.2 \mu\text{g m}^{-3}$  for Paris and  $2.9 \mu\text{g m}^{-3}$  for Rambouillet), further considered as background, while samples from July 11 to 13 and July 17 to 19 (Fig. 2) were representative of polluted conditions as their concentrations were higher than the mean value. Such OC variations were consistent with higher concentrations of  $\text{O}_3$ ,  $\text{NO}_x$  and  $\text{SO}_2$  for the pollution periods compared to the background one (Fig. 2). The different periods of pollution were also characterized by the contribution of different air masses (Figure 2) arriving from north-west for Paris and varied contributions to Rambouillet. Backward trajectories were calculated for 24 hours for the Rambouillet site with the HYSPLIT model (Stein et al., 2015) using the Global Data Assimilation System (GDAS) for 1 degree resolution. Those highlights the contribution of different air masses during the background and pollution periods. As observed in Fig. S2, during the background period (July 03) air masses arriving from the northwest shows maritime and continental contributions. During the pollution period (July 12), air masses arrive from northeast, crossing urban dense populated areas of Belgium and Paris city. During the second period of pollution (July 17 to 19), higher temperatures, OC concentrations and an atypical event of long-range transport of biomass burning emissions from the south-west of France on July 19 were also reported (Menut et al., 2023). In agreement, back-trajectories analysis highlight

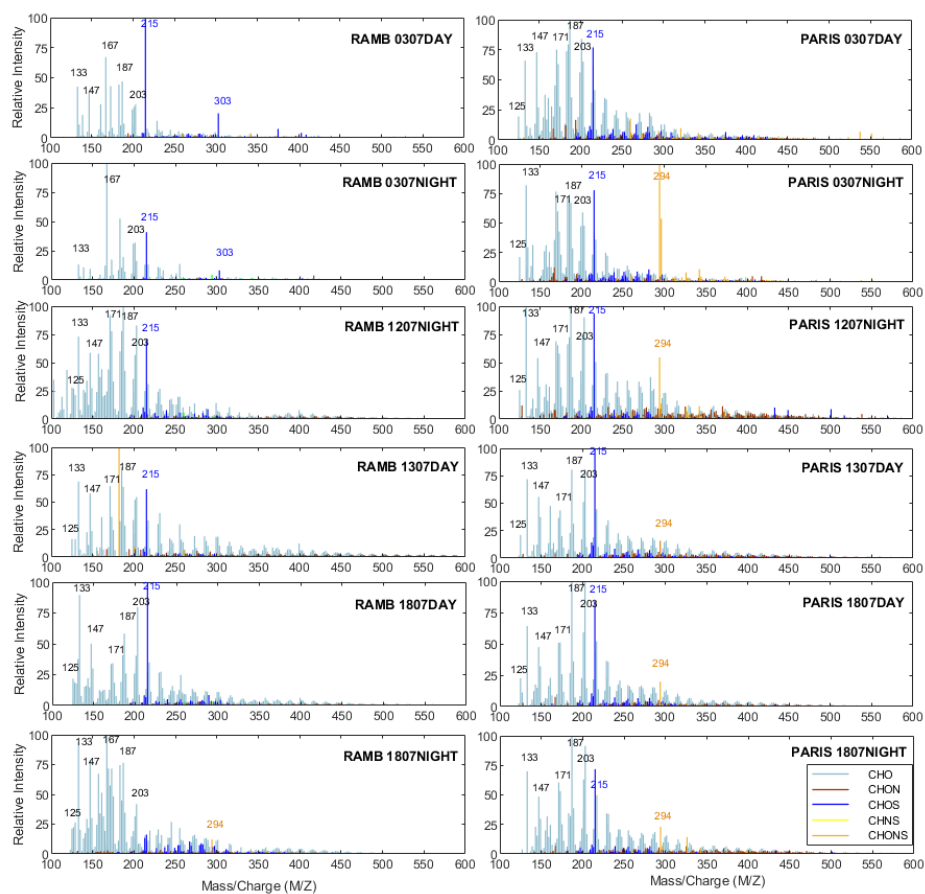
Mis en forme : Couleur de police : Texte 1

the arrival of air masses from the south of Paris, showing that inside the second period, the aerosols may be influenced by different chemical processes and sources.

### 3.2 Molecular composition

HRMS analysis for day and night samples from the urban and forested area of Paris were compared to investigate differences and similarities in the particle chemical composition at both sites. The mass spectra of specific samples representing the background (July 3 and 4) and polluted periods (July 11 to 13 and July 17 to 19) are summarized in Fig. 3. Between 163.944 and 504.133 elemental formulae were identified with molecular weights mostly distributed below 600 m/z. It is important to highlight the lower number of molecular formulae assigned in the background samples of July 3 for Rambouillet site, with 163.944 and 207.699 formulae for day and night samples (Table S1).

Considering analysis performed on different urban and rural environments, we suggest possible compounds that can be associated to the molecular formulae identified in this study, however they could also be associated to other isomers. A predominant signal observed at 215.023 m/z in all samples for C<sub>5</sub>H<sub>12</sub>SO<sub>7</sub> is compatible with an isoprene oxidation product as suggested by Zherebker et al. (2024). C<sub>10</sub>H<sub>17</sub>NSO<sub>7</sub> formula at 294.065 m/z is compatible with an  $\alpha$ -pinene oxidation product formed under the presence of NO<sub>x</sub> and SO<sub>2</sub> (Surratt et al., 2007, 2008), showing a higher relative intensity during the night period at Paris. This organosulfate has been previously detected in the field (Kourtchev et al., 2014; Kourtchev et al., 2016; Giorio et al., 2019; Wang et al., 2022), and may highlight the influence of anthropogenic pollutants on SOA formation when mixed with biogenic compounds as it is formed in the presence of the anthropogenic pollutants NO<sub>x</sub> and SO<sub>2</sub>. The dependence on organosulfate formation in the presence of anthropogenic species has been followed during the oxidation of monoterpenes and isoprene. The presence of acidic sulfate seeds (Iinuma et al., 2009; Surratt et al., 2007) and additional presence of NO<sub>x</sub> species for the nitroxy types (Surratt et al., 2008) were observed. The mechanisms proposed for organosulfates formation involves sulfate species reactions via epoxide formation, esterification, aqueous reactions or direct reaction with gaseous SO<sub>2</sub> (Brüggemann et al., 2020). While nitrate radical chemistry was suggested to determine nitroxy organosulfates formation (Iinuma et al., 2007). It is important to consider that in Rambouillet, NO<sub>x</sub> and SO<sub>2</sub> levels and sulfur compounds affecting this chemistry can be also influenced by microbial activity (Andersen et al., 2024). Although we cannot attribute the molecular formula C<sub>7</sub>H<sub>12</sub>O<sub>11</sub>S at 303.003 m/z, the fact that it appears only in Rambouillet samples may suggest a biogenic origin.



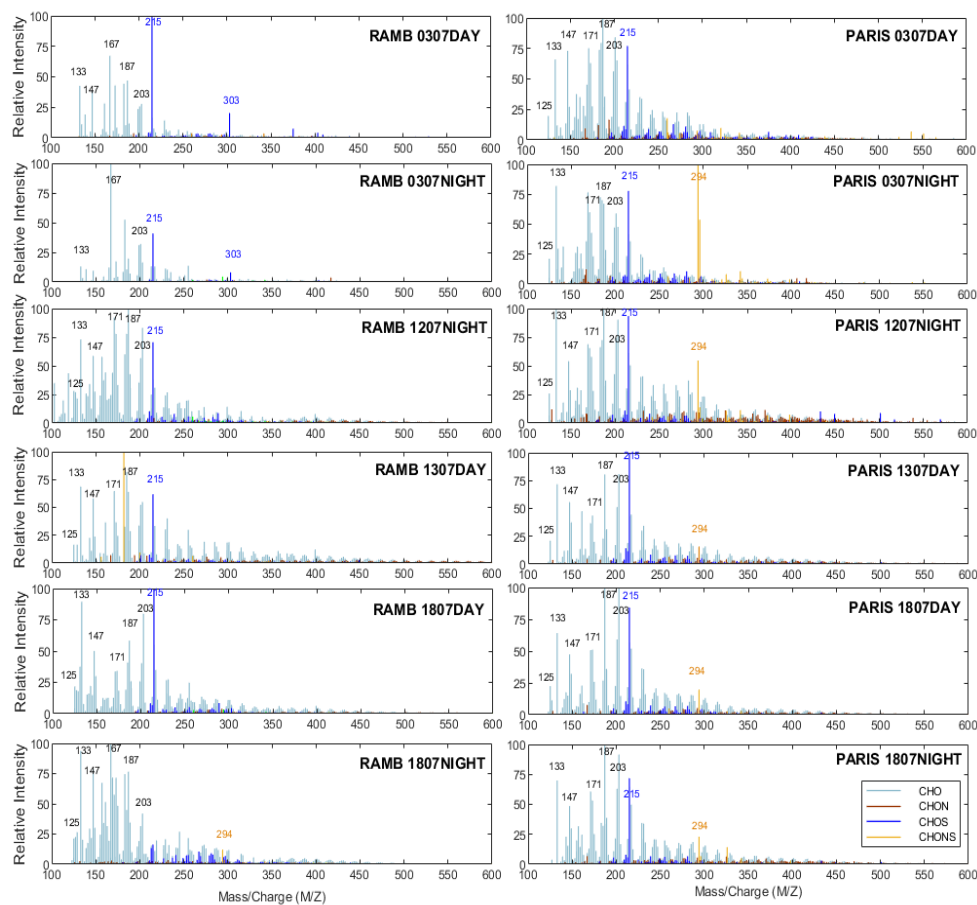


**Figure 3:** Reconstructed mass spectra for specific consecutive samples of Rambouillet (RAMB) and Paris. Different colors show the compound classes CHO (clear blue), CHON (brown), CHOS (dark blue), CHNS (yellow), CHONS (orange). Samples here represent examples of the background period (July 3) and pollution periods (July 12, 13, and 18) from day and night measurements performed during the summer 2022.

Peaks  $133.014\text{ m/z}$  ( $\text{C}_4\text{H}_8\text{O}_5$ ),  $147.030\text{ m/z}$  ( $\text{C}_5\text{H}_8\text{O}_5$ ),  $167.071\text{ m/z}$  ( $\text{C}_9\text{H}_{12}\text{O}_3$ ),  $171.066\text{ m/z}$  ( $\text{C}_8\text{H}_{12}\text{O}_4$ ),  $187.061\text{ m/z}$  ( $\text{C}_8\text{H}_{12}\text{O}_5$ ) and  $203.057\text{ m/z}$  ( $\text{C}_8\text{H}_{12}\text{O}_6$ ) appeared at high relative intensities in all samples. These CHO compounds may have anthropogenic or biogenic origins (Kourtchev et al., 2014). For example,  $\text{C}_8\text{H}_{12}\text{O}_4$ , and  $\text{C}_8\text{H}_{12}\text{O}_6$  are compatible with terpenylic

365 acid, and 3-methyl-1,2,3-butanetricarboxylic acid (MBTCA) as oxidation products of  $\alpha$ -pinene ozonolysis (Kristensen et al., 2013, 2014; Yasmeen et al., 2010). Oxidized low-molecular weight compounds such as  $C_4H_6O_5$  and  $C_5H_8O_5$  may be associated with carboxylic acids such as malic acid and hydroxyglutaric acid (Daellenbach et al., 2019). While malonic acid has been observed in the photo-oxidation scheme of toluene (Sato et al., 2007), hydroxyglutaric acid may be formed from monoterpene oxidation under the presence of  $NO_x$  (Claeys et al., 2007; Zhang et al., 2018). The presence of  $C_8H_{12}O_5$  was observed by 370 Kourtchev et al. (2016) in the Amazon forest with samples influenced by biogenic emissions and biomass burning.  $C_9H_{12}O_3$  it can be related to pinene oxidation product.

Additionally, an increase in the relative intensity of  $C_6H_5NO_4$  at 154.015  $m/z$  is observed on July 19 (Fig. S32) in the day-time samples at high relative intensities of 21.8% and 19.2% for Paris and Rambouillet, while its relative intensity is lower than 4% and 1.8%, respectively, in the remaining samples.  $C_6H_5NO_4$  has been previously assigned as nitrocatecols (Kourtchev et al., 375 2016), and attributed to biomass burning (Iinuma et al., 2010). This relative intensity variability between samples together with higher OC and  $NO_x$  concentrations for that particular day supports this attribution, and confirm in agreement with Menut et al. (2023) that different chemical processes occurred during this fire event.

In order to provide additional information of the chemical diversity of the aerosol samples, the percentage of formulae number per compound families CHO, CHON, CHOS, CHNS and CHONS are reported in Fig. 4Table-2. The number of formulae 380 associated to each group are detailed in Table S1. Samples under study were characterized by higher number of formulae from CHO and CHON compounds (>26%) and lesser of CHOS and CHONS compounds. CHO and CHON showed percentage of number formulae between 30.29.5% to 45.4.4% and 26.3% to 49.8.2% in Rambouillet, while in Paris varied between 28.6.8% to 44.3.6% and 36.5.8 to 53.0%, respectively. Although molecular classes may show a seasonal variation due to the contribution of different sources (Daellenbach et al., 2019), a high abundance of CHO and, especially, CHON fractions at areas influenced 385 by urban emissions observed here is consistent with some previous studies (Wang et al., 2018; Giorio et al., 2019; Daellenbach et al., 2019) that reported HRMS analysis of samples collected in urban environments.

Samples collected on July 3 and 4 in the forest area presented a higher percentage of number formulae of CHOS compounds (>17%) than those collected in urban Paris (>10.2%). For those days, Paris samples have CHON presence higher than 43.0%, which was larger than CHO (<34.3.3%) while Rambouillet showed an opposite tendency. Besides those samples, CHON 390 assignments either dominate or remain close to CHO assignments, except for July 19. The presence of sulfur containing compounds (CHOS) has shown the role of oxidizing biogenic SOA in different remote areas which can be influenced by anthropogenic emissions such as Manaus in the Amazon forest (Kourtchev et al., 2016) or Hyytiälä in the Boreal forest (Daellenbach et al., 2019).

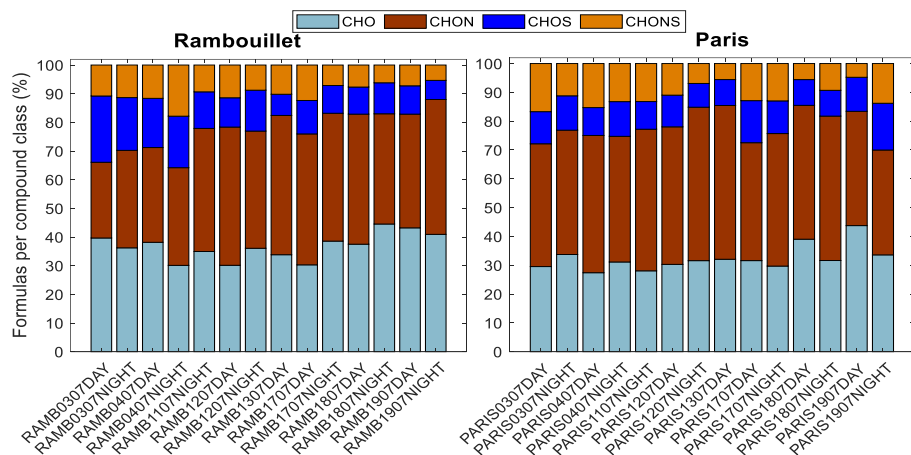


**Figure 4: Comparison of the percentage of number of formulas per compound class for Rambouillet (RAMB) and Paris samples. Different colors show the compound classes CHO (clear blue), CHON (brown), CHOS (dark blue), and CHONS (orange).**

**Table 2. Compound-classes and aromaticity-equivalent Xc-based-classes contribution for PM<sub>1</sub> samples collected during the summer 2022 at Paris and Rambouillet (RAMB) derived by HRMS. The percentage of number of formulas per compound class and per aromaticity equivalent are calculated in function of the total number of formulae. The OC and EC concentrations were obtained by thermal-optical analysis.**

sample name	Number of formulas per compound class detected <sup>a</sup> (%)					Concentration (µg m <sup>-3</sup> )		Number of formulas per aromaticity equivalent class <sup>b</sup> (%)		
	CHO	CHON	CHOS	CHNS	CHONS	OC	EC	unsaturated	aromatic	condensed
RAMB0307 DAY	39.5	26.3	23.1	0.3	10.8	1.3	0.0	50.4	34.3	15.4
RAMB0307 NIGHT	35.8	33.6	18.2	1.1	11.2	1.2	0.0	38.4	38.6	23.0
RAMB0407 DAY	38.0	32.9	17.1	0.5	11.6	1.8	0.1	48.1	34.6	17.3
RAMB0407 NIGHT	29.8	33.7	17.8	1.0	17.7	-	-	43.2	38.0	18.7
RAMB1107 NIGHT	34.6	42.5	12.6	1.0	9.3	3.5	0.2	41.5	38.4	20.1
RAMB1207 DAY	29.5	47.2	10.0	2.2	11.2	3.0	0.2	32.8	33.2	34.0
RAMB1207 NIGHT	35.5	40.2	14.0	1.6	8.6	4.7	0.2	31.0	33.5	35.5
RAMB1307 DAY	33.5	48.2	7.3	0.9	10.1	4.2	0.2	33.6	32.2	34.1
RAMB1707 DAY	30.0	45.2	11.5	1.1	12.2	3.1	0.2	37.5	35.6	26.9
RAMB1707 NIGHT	38.1	44.0	9.5	1.3	7.1	4.2	0.2	35.7	35.9	28.4
RAMB1807 DAY	37.3	45.2	9.4	0.5	7.7	3.9	0.2	35.2	34.9	29.8
RAMB1807 NIGHT	44.4	38.3	10.8	0.3	6.2	5.5	0.2	33.2	34.4	32.4

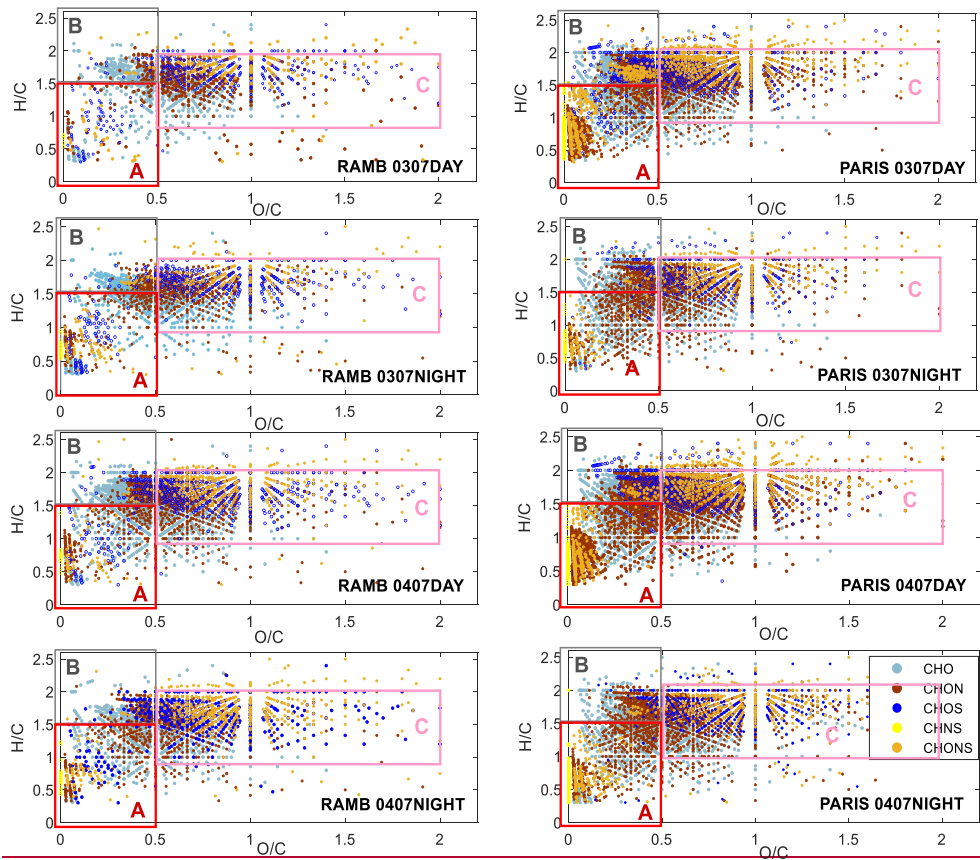
RAMB1907 DAY	43.0	39.5	9.8	0.5	7.2	7.7	0.3	33.7	34.0	32.3
RAMB1907 NIGHT	40.9	46.9	6.7	0.2	5.3	4.6	0.3	33.0	39.8	27.2
PARIS0307 DAY	28.9	41.7	10.9	2.2	16.3	2.0	0.2	41.3	28.9	29.8
PARIS0307 NIGHT	33.3	42.5	11.8	1.4	11.0	2.0	0.2	45.4	21.4	33.3
PARIS0407 DAY	26.8	46.6	9.5	2.2	14.9	2.5	0.3	40.9	30.4	28.8
PARIS0407 NIGHT	30.5	42.7	11.8	2.2	12.9	2.3	0.2	45.2	30.5	24.3
PARIS1107 NIGHT	27.7	48.5	9.5	1.3	13.0	-	-	41.7	33.4	24.9
PARIS1207 DAY	29.8	47.0	10.8	1.6	10.8	3.2	0.5	40.9	34.2	24.9
PARIS1207 NIGHT	31.3	52.8	8.2	0.9	6.8	5.9	1.1	39.8	35.9	24.3
PARIS1307 DAY	31.9	53.0	8.9	0.6	5.5	5.0	1.2	39.8	35.6	24.5
PARIS1707 DAY	31.1	40.2	14.4	1.7	12.7	3.2	0.3	45.1	32.8	22.1
PARIS1707 NIGHT	29.2	45.2	11.1	1.8	12.7	4.9	0.9	38.3	32.0	29.7
PARIS1807 DAY	38.7	46.0	8.8	1.0	5.5	4.3	0.9	40.4	35.5	24.1
PARIS1807 NIGHT	31.2	49.4	8.8	1.4	9.2	5.7	1.2	34.2	32.5	33.4
PARIS1907 DAY	43.6	39.6	11.8	0.3	4.8	10.0	1.2	36.0	34.8	29.3
PARIS1907 NIGHT	33.0	35.8	16.0	1.7	13.6	7.8	0.5	36.7	33.2	30.1

<sup>a</sup> Values represent the percentage of different subgroup among the total number of assigned formulas per each sample.

<sup>b</sup> Values represent the percentage of different subgroups after classification based on aromaticity equivalent ( $X_c$ ) following Yassine et al. (2014).

The fact that similar percentage of molecular classes together with similar OC concentrations are observed in this work ~~shows a similar chemical composition~~ for most of the days for the periods of pollution ~~at two locations of the Paris region, may suggest similar aerosol sources influencing the chemical composition~~. This is not observed for the background period in the Rambouillet forest as a lower number of molecular formulae of CHON compounds were observed, as a consequence of the lower influence of anthropogenic emissions.

3.2.1 Elemental ratios Aromaticity analysis





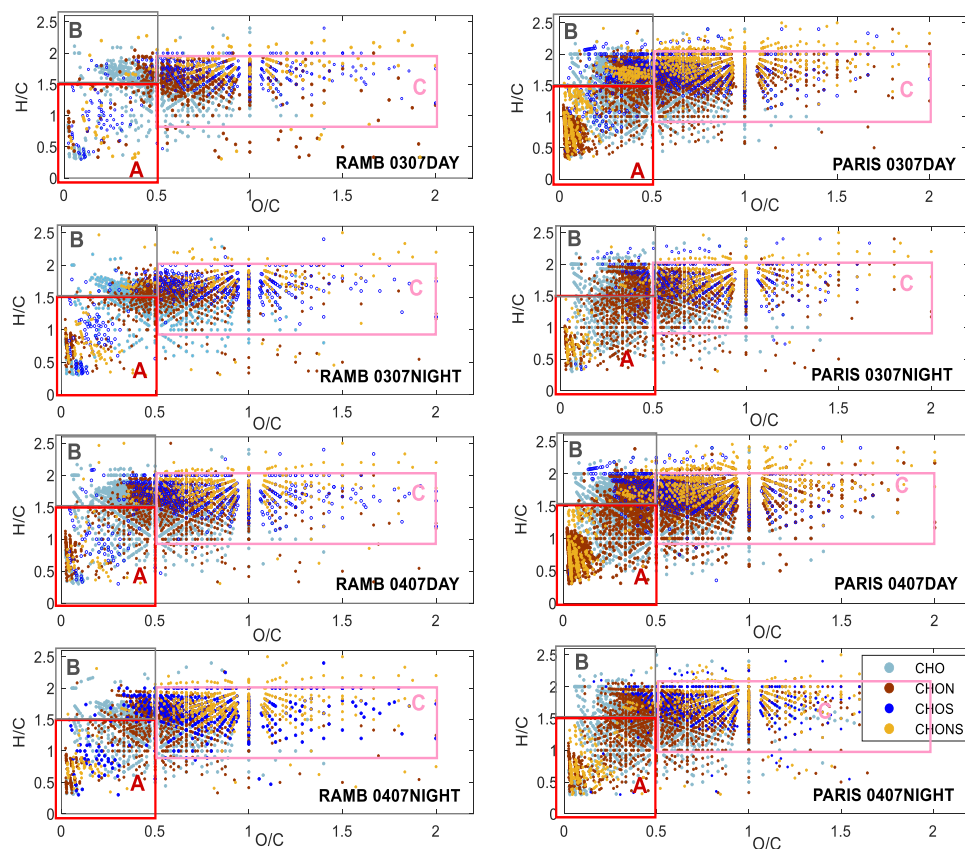


**Figure S4:** Van Krevelen diagrams for different compound classes of samples collected during day and the night periods on July 3 and 4 in Rambouillet and Paris during the summer 2022. Region A represents the low oxygenated aromatic hydrocarbon domain, region B the aliphatic domain and region C the more oxidized domain.

Figure S43 shows the visual resemblance of VK diagrams for samples collected for the same days in the urban and the forested areas, with high density of compounds with  $O/C < 1$  and  $H/C < 2$ . Samples from Paris and Rambouillet were influenced by the presence of low oxidation aromatic compounds and higher oxidized molecules. Similarities in the VK for most of the samples and between the sites suggests a general consistency of aerosol sources between different days. Small differences on the density of peaks between samples were observed for July 3 and 4, therefore, their VK diagrams in function of the compound classes are better explored in Fig. S4.

Paris samples showed a higher density of low oxygenated aromatic compounds (region A) with main contributions of CHO, CHON and CHONS families, while Rambouillet shows to be less influenced by N containing families in region A during these dates. Similarly, in region C, represented by more oxidized aerosol, the presence of CHONS compounds, especially for day samples, was abundant for the urban area. Besides those samples, both sites showed similar patterns at region A for the pollution periods. Similarly, region B (aliphatic) showed a lower density of compounds at Rambouillet during the background periods. A predominance of CHO and CHOS contributions, which can be associated to biogenic or anthropogenic first generation products (Kourtchev et al., 2013), was observed. At Paris, an increase on the density of CHONS compounds in region B compare to Rambouillet was observed, especially for samples collected during the day. a similar influence of aromatic compounds, which is better investigated in the following section.

Although the complexity of the organic mixtures of samples collected in the field with a wide contribution of different aerosols, some patterns previously observed in the literature may suggest the compatibility of some sources in Fig. 5. For example, possible contributions of mono and dicarboxylic acids at the aliphatic domain and soot derived materials or oxidized polycyclic aromatic hydrocarbons PAHs in the aromatic domain (Wozniak et al., 2008; Lin et al., 2012), the presence of lipids and fatty acids in aliphatic domain and condensed hydrocarbons observed in plants (Giorio et al., 2015), and influence of fresh and oxidized biogenic emissions (monoterpenes, limonene, isoprene,  $\Delta_3$  carene) for more oxidized aerosols (Kourtchev et al., 2015). Those compounds could be originated from anthropogenic sources such as vehicular emissions, which can contribute for example, with nitroaromatic compounds formation. Also, contributions of biogenic sources resulting from the oxidation of terpenes and isoprene originated in forested areas with oaks and pines population.

### 3.2.2 Aromaticity Analysis

Although H/C and O/C values suggested the presence of low oxygenated aromatic compounds (Koch and Dittmar, 2006; Mazzoleni et al., 2012), VK diagrams do not provide further structural information and relying only on H/C and O/C values could be a non-accurate metric for the analysis of aromatic compounds. Due to the similar density of signals falling in the region of low oxygenated aromatic compounds showed in the VK diagrams in the forested area of Rambouillet and the urban area of Paris for samples after July 4 (Fig. S3), the aromaticity equivalent ( $X_c$ ) of the aerosol samples were calculated following Yassine et al. (2014). They were grouped as unsaturated, aromatic, and condensed aromatic compounds and reported in percentages of the total number of formulae as shown in Fig. 6Table 2. Differences in the number contribution of unsaturated, aromatic, and condensed aromatic compounds were observed mainly at samples from the background period in samples from (July 3 and 4), where the condensed aromatic compounds at Rambouillet contribute from 15.4% to 223.0% while higher contributions were observed in Paris, 204.3% to 2833.2%. An opposite trend was observed between July 12 and 13, where condensed aromatics were more concentrated at Rambouillet than Paris, which had slightly higher contributions of unsaturated compounds. Besides the samples of the beginning of July, strong differences in the aromaticity were not observed in terms of  $X_c$ . At comparing the variations on the percentage number of formulae for the same site, we observed an increase in the condensed fraction from the background to the pollution site for Rambouillet. Although similar OC concentrations were

observed at both sites. We observed differences into the chemical composition, especially at Rambouillet site during the background period. Here, the average conditions highlight the lower number of formulas per aromaticity class for condensed compounds, probably from aromatic origin. While similar percentage of number of formulae were averaged for the pollution periods at both sites (Fig. S5) with average values of 40%, 34% and 26% for Paris and 35%, 36% and 29% for Rambouillet of unsaturated, aromatic and condensed classes respectively.

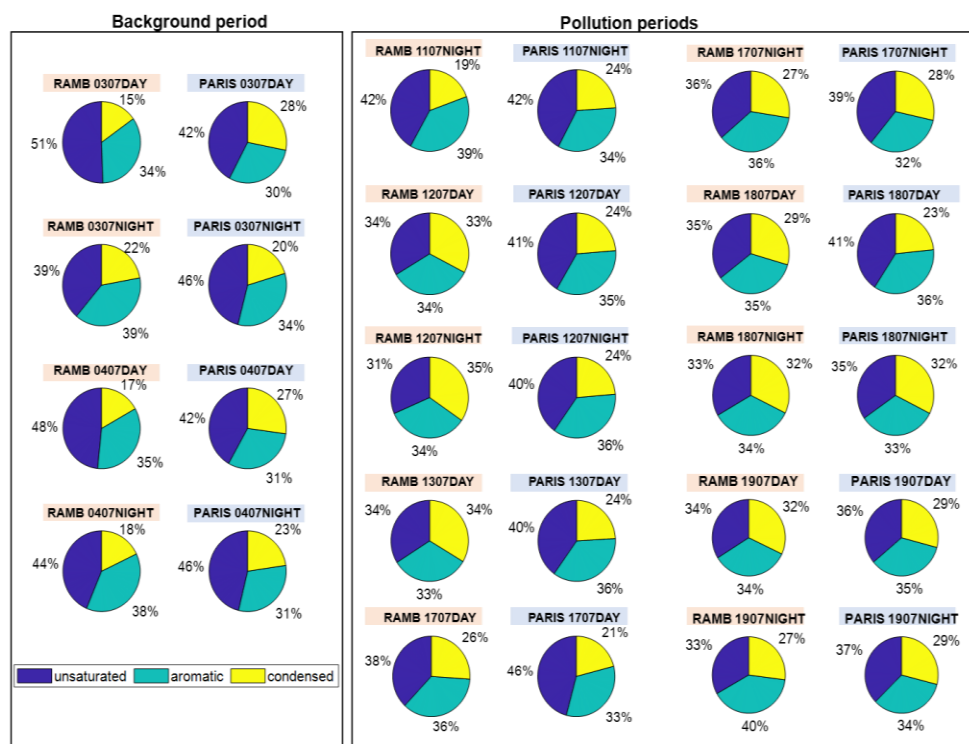


**Figure 6: Comparison of the percentage of number of formulas per aromaticity equivalent at Rambouillet (RAMB) and Paris samples. Different colors show the compound classes unsaturated (dark blue), aromatic (clear blue) and condensed (yellow).**

Aromatic compounds are mostly observed in areas strongly influenced by traffic emissions in the summer (Kourtchev et al., 2014). The lower number of aromatics observed at Rambouillet samples of July 3 and 4 may reflect in a better way the biogenic

nature of emissions observed in a forested area under weak urban influence, also demonstrating the background signature of this period. The difference between these samples and the others is also verified by the cosine differences higher than 0.3, observed in Fig. S64, especially for samples collected during nighttime. These observations, together with the similarities on the OC concentrations and the contribution of CHON compounds observed above, may suggest air masses arrival from urban areas to this forested environment during the sampling period. A confirmation of inputs of air masses with urban/ industrial contributions from Paris, Brussels and the Ruhr region to the forested area of Rambouillet was recently reported during the ACROSS campaign by Andersen et al. (2024).

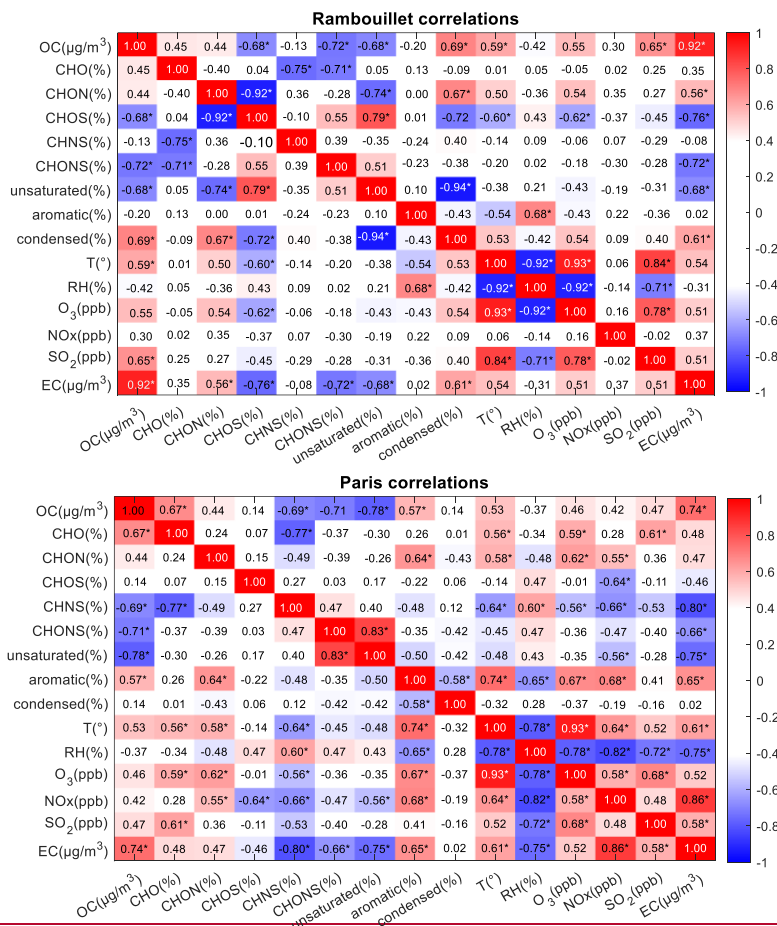
### 3.3 Influence of chemical classes and meteorological parameters on OC concentrations

The mean values of meteorological parameters (T and RH), and of anthropogenic pollutants concentrations ( $O_3$ ,  $NO_x$ ,  $SO_2$  and EC) were considered over the sampling period (Table S1) to evaluate their influence on the chemical composition of the OA through correlation analysis. The correlation coefficients (r) observed for Paris and Rambouillet are summarized in Fig. 75. Only statistically significant correlations (i.e. p value < 0.05) with good and moderate linear positive/negative coefficient values are discussed ( $-0.40 < r < 0.40$ ). Figure 75 showed good positive correlations between T and OC concentrations, especially for Rambouillet samples ( $r = 0.59$ , p-value = 0.03). The temperature may influence OC concentrations, affecting primary and secondary processes such primary OA emissions, precursor emissions (Sheehan and Bowman, 2001), boundary layer height, and circulation patterns (Zhang et al., 2023). These factors may affect daily variations of different compounds and in turn the OC concentration, which is observed here by the different temperature effect on the chemical families. RH was negatively correlated with  $NO_x$  ( $r = -0.82$ , p-value < 0.001) and EC ( $r = -0.75$ , p-value = 0.003) in Paris. This was not the case for Rambouillet, where  $NO_x$  and EC levels were lower and instead only negative correlations with  $SO_2$  ( $r = -0.71$ , p-value = 0.006) were observed. The lack of correlation between the meteorological conditions and pollutants in Rambouillet can be a consequence of the lack of local anthropogenic emissions in the forested site, which is supported by the low levels of EC observed. In the presence of humidity  $NO_x$  and  $SO_2$  gases can transition into acidic species, decreasing their concentration and therefore, being negative correlated with RH.

The presence of ~~these~~ anthropogenic pollutants can influence the formation of certain compounds as observed for the percentage number of molecular formulae for CHON, which was positively correlated with  $NO_x$  concentrations ( $r = 0.565$ , p-value = 0.0595) in Paris samples. CHO compounds can undergo  $O_2$  oxidation, forming alkylperoxy radicals ( $RO_2\cdot$ ), and subsequent  $NO_2$  addition or NO reaction, leading to the formation of N-families (e.g., organo-nitrate, peroxyxynitrate) (Atkinson, 2007; Kroll and Seinfeld, 2008). Therefore, in urban environments,  $RO_2\cdot$  reactions with  $NO_x$  represent an important pathway for SOA formation. The fact that  $NO_x$  and CHON are positively correlated only in Paris highlights the formation of those compounds on urban environments. Following this oxidation scheme, aromatic compounds are able to form nitro-aromatic compounds (Sato et al., 2022), showing also a good correlation between the aromatic subgroup and  $NO_x$  in Paris ( $r = 0.68$ , p-value = 0.01). The fact that the chemical family's correlations with the anthropogenic pollutants follow different tendencies for both sites may suggest that some species are formed in the urban area and then transported to the forested site.  $NO_x$  was also

negative correlated with the percentage number of formulae for CHOS, CHONS, and unsaturated types, showing they those compounds can react in the presence of this anthropogenic pollutant, known as a major oxidant, especially during the night (Atkinson and Arey, 2003). ~~and SO<sub>2</sub> are involve into the formation of CHOS and CHONS compounds. Although, non-~~  
statistically significant correlations were observed for those pollutants and the percentage number of molecular formulae for CHOS and CHONS, their influence have been reported (Surratt et al., 2008) and was observed here through the detection of compounds such as the C<sub>5</sub>H<sub>12</sub>SO<sub>2</sub> and C<sub>10</sub>H<sub>12</sub>NSO<sub>2</sub> (Section 3.2).

It is important to highlight the different role of RH into the chemical families as a ~~positive correlation~~ negative correlation was observed with the percentage of number formulae for aromatic compounds in Paris (r= -0.65, p-value=0.01), while the opposite was observed in Rambouillet (r= 0.7068, p-value= 0.01) and with CHOS family in Paris (r= 0.63, p-value= 0.02). Differences were also observed for correlations between the percentage number of molecular formulae for different families for each site. For example, CHO were negative correlated with ~~CHONS~~ (r= -0.71, p-value= 0.006) and ~~CHON~~ with CHOS (r= -0.7392, p-value< 0.0074) in Rambouillet. In Paris, aromatics were positively correlated with CHON families (r= 0.7364, p-value= 0.0042) and EC concentrations (r= 0.65, p-value= 0.02), which was not the case of Rambouillet. The lack of correlation between EC and aromatics for Rambouillet may suggest the depleted of aromatic compounds. These differences between sites are an indicative of the different processes occurring in each environment. Negative correlations observed at both sites between the percentage number of molecular formulae for CHO and CHONS families highlighted further oxidation processes under the presence of anthropogenic oxidants such as SO<sub>2</sub> and NO<sub>x</sub>. ~~Negative correlation between the percentage number of molecular formulae for CHOS and CHON can indicate competitive reactions for the oxidation of different VOC precursors.~~



Mis en forme : Normal, Gauche

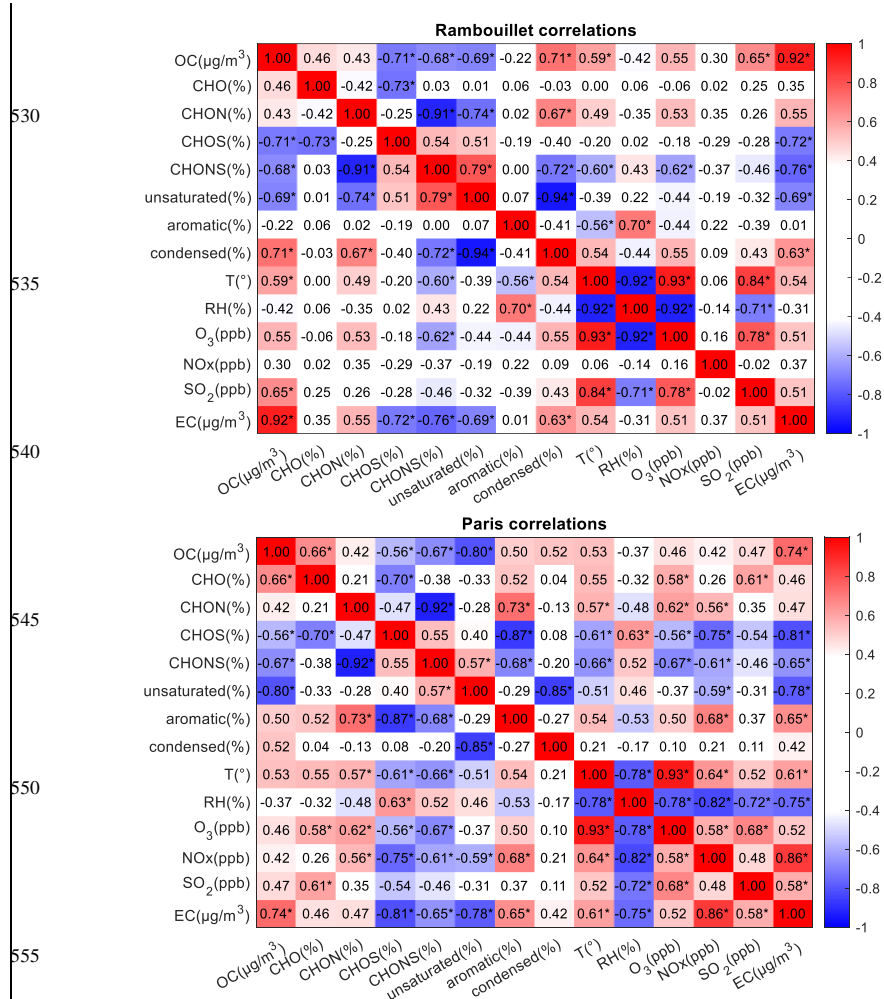


**Figure-7:** Correlation coefficient matrix for compounds classes (CHO, CHON, CHOS, CHONS and CHONS), meteorological conditions (T and RH), anthropogenic pollutants (O<sub>3</sub>, NOx, SO<sub>2</sub> and EC) and OC concentrations observed for Rambouillet (up panel) and Paris (bottom panel). The Pearson correlation coefficients for negative correlation (blue) and positive correlations (red) are presented here. \* shows statistically significant (p-value < 0.05) correlation values.

O<sub>3</sub> may play different roles as photochemistry indicator as for example, good negative correlation with the percentage number of molecular formulae for CHOS ( $r = -0.5662$ ,  $p\text{-value} \leq 0.053$ ) ~~was observed for Rambouillet~~, while positive correlations were observed for the percentage number of molecular formulae for CHO ( $r = 0.589$ ,  $p\text{-value} < 0.04$ ) and CHON ( $r = 0.62$ ,  $p\text{-value} < 0.032$ ) in Paris. O<sub>3</sub> is an important oxidant for biogenic precursors, but it can also correlate to other day and night oxidants such as OH and NO<sub>3</sub>, respectively. The influence of NO<sub>x</sub> and O<sub>3</sub> to promote the aerosol formation was also observed at the molecular scale in Fig. S75, for common formulae (577) from different families of compounds at both Paris and Rambouillet. In Figure S75., NO<sub>x</sub> concentration is positively correlated with percentage of number formulae for compounds in the low-oxygenated aromatic domain, while O<sub>3</sub> influence the more oxidized region, which seems also positively correlated with the OC concentrations, highlighting the importance of the secondary contribution to OA formation.

#### 4 Comparison of the chemical composition

This work aimed to provide the description of chemical composition of the organic fraction of the aerosol to investigate the differences in PM<sub>1</sub> collected in the urban and forested areas of Paris from day and night measurements during the summer 2022. Lower values of OC together with lower NO<sub>x</sub> concentrations observed during the background period highlighted an atmosphere less influenced by anthropogenic inputs in the forested area. For the defined polluted periods, similar aerosol chemical compositions were observed for both urban and forested areas with OC concentration values in agreement with previous studies carried out in the Paris region (Bressi et al., 2013; Lanzafame et al., 2021).

The presence of NO<sub>x</sub>, CHON and CHONS species, aromatic and condensed aromatic compounds detected in Rambouillet samples together with the air mass back-trajectories previously reported highlight the impact of urban inputs in forested areas. Similarly, it should also be noted the important density of peaks probably associated to biogenic contributions identified in the Paris center samples (e.g., C<sub>8</sub>H<sub>12</sub>O<sub>4</sub>, C<sub>8</sub>H<sub>12</sub>O<sub>6</sub>, C<sub>10</sub>H<sub>17</sub>NSO<sub>7</sub>). As wind directions from north-east and west were observed for Paris during the sampling period, the detection of biogenic compounds may be either influenced by biogenic VOC emissions from natural areas close to the sampling site (e.g., Vincennes and Boulogne forests or urban trees) or by direct biogenic aerosol inputs. This observation is consistent with previous studies showing that biogenic compounds can play an important role during the summer in urban areas (Amarandei et al., 2023; Giorio et al., 2019; Maison et al., 2024).

The five molecular classes (CHO, CHON, CHONS, CHOS, and CHNS) identified in this work may originate from both biogenic and anthropogenic sources, influencing both background and the pollution periods. The different compound classes show a predominance of CHO (>26.8%) and CHON (>26.3%) groups, consistent with reported contributions in the literature: 25.2% and 47.7% in Padua (Italy) (Giorio et al., 2019), 45.2% and 20.9% in Iasi (Romania) (Amarandei et al., 2023), 44% and 21% in Beijing (China) (Wang et al., 2018) while 32% and 35% in Mainz (Germany) (Wang et al., 2018). These similarities suggest the ubiquitous contribution of some aerosols component both from anthropogenic and biogenic origin in urban areas. Although no significant difference was observed for OC concentrations between daytime and nighttime, the higher relative intensity of isomeric compounds such as C<sub>10</sub>H<sub>17</sub>NSO<sub>7</sub> (more prominent in the Paris area) highlights the different processes and sources and potential variations of species concentrations during the day. [The description of the OA chemical composition at](#)



molecular scale improves the understanding between the mixing of biogenic and anthropogenic emissions as for example, organosulfur compounds such as  $C_5H_{12}SO_7$  and  $C_{10}H_{17}NSO_7$  were detected. Those have been previously observed in environments influenced by urban emissions (Kourtchev et al., 2014; Kourtchev et al., 2016; Giorio et al., 2019; Wang et al., 2022) showing the impact of mixed anthropogenic-biogenic air masses. Interactions between different biogenic and anthropogenic components (Rattanavaraha et al., 2016; McFiggans et al., 2019; Shrivastava et al., 2019) were previously reported to influence the OA composition and formation efficiency. Additionally, although only direct infusion analysis was performed in this work, the detection of molecular formulae compatible with those of the literature for possible biogenic (e.g.  $C_8H_{12}O_4$  and  $C_8H_{12}O_6$ ) (Kristensen et al., 2013, 2014) and anthropogenic compounds (e.g.  $C_6H_5NO_4$ ) (Iinuma et al., 2010) highlight the importance of providing the chemical composition at molecular scale as organic tracers can be detected. Those can be later associated to specific SOA precursors and formation pathways. As observed, molecular scale information provides fingerprints on the organics composition in the Paris megacity and a forested area. The detection of compounds likely associated to biogenic (e.g.  $C_8H_{12}O_4$  and  $C_8H_{12}O_6$ ) (Kristensen et al., 2013, 2014) and anthropogenic (e.g.  $C_6H_5NO_4$ ) (Iinuma et al., 2010) oxidation products highlights the importance of understanding urban and rural chemistries at the molecular level to accurately identify aerosol sources. Additionally,  $C_5H_{12}SO_7$ ,  $C_{10}H_{17}NSO_7$  and  $C_8H_{12}O_5$  compounds, previously observed in environments influenced by urban emissions (Kourtchev et al., 2014; Kourtchev et al., 2016; Giorio et al., 2019; Wang et al., 2022) demonstrates the impact of mixed anthropogenic-biogenic air masses, which can lead for example to the formation of organosulfur compounds. Given that the interactions between different biogenic and anthropogenic components (Rattanavaraha et al., 2016; McFiggans et al., 2019; Shrivastava et al., 2019) have been shown to influence the OA composition and formation efficiency.

Similarities found in the particle chemical composition on the samples under study derived from HRMS analysis and the temporal series of OC and  $O_3$  concentrations for the pollution periods highlights a homogeneity (source consistency) in the OA composition for both urban and forested areas of Paris when anthropogenic emissions increases, consistently with previous observations of aerosol composition for urban, suburban and rural Parisian areas (Bressi et al., 2013). These observations show that forested areas can be affected by anthropogenic inputs, influencing the atmospheric chemical composition and therefore their impact on the OA budget and related processes.

## 5 Conclusions

Aerosol filter sampling was performed during the ACROSS intensive campaign at two sites in greater Paris area during the summer 2022 to investigate the chemical composition of the organic fraction of  $PM_{10}$  at the molecular scale at two sites representative of urban (Paris) and forested (Rambouillet) environments. The OC concentrations derived in this work were similar for both sampling sites, and in agreement with values previously reported for Paris region, suggesting the influence of the urban inputs in the suburban forested area of Rambouillet. HRMS analysis showed similar patterns of the contributions of anthropogenic and biogenic emissions on both sites for periods of pollution. This was not the case for samples of the

background period on July 3 and 4, more representing the local emissions at both sites, i.e. highlighting biogenic contributions at Rambouillet and anthropogenic sources at Paris. This observation was confirmed by statistical analysis, which showed the influence of different process occurring at both sites, together the aromaticity analysis, which shows a higher presence of condensed aromatic compounds in Paris than in Rambouillet with a higher density of peak assignments in the VK diagrams. The high number contribution of CHO and CHON families in both [sites](#) verified the aerosol sources homogeneity for periods of pollution. [Similar OA composition observed at the urban and forested areas of the Paris region during such periods reflects anthropogenic and biogenic emissions interactions enhancing summertime aerosol formation. This observation depicts a progressive impact of densely populated areas \(megacities\) into rural/ forested areas with increasing emissions.](#) Additionally, the detection of tracers such as  $C_3H_{12}SO_7$  and  $C_{10}H_{17}NSO_7$  and  $C_6H_5NO_4$  observed at both sites completes this statement, showing the contribution of mixed biogenic emissions and biomass burning sources and highlights the importance of using molecular tracers in the description and quantification of the organic fraction of the aerosol.

#### Data availability

Data presented in this work for the two sampling sites are available at the AERIS (French national center for atmospheric data and services) facility (<https://across.aeris-data.fr/catalogue/>). Data set already available are: OC and EC concentrations for Paris (Pereira et al., 2024a) and Rambouillet (Pereira et al., 2024c), HRMS analysis for Paris (Pereira et al., 2024b) and Rambouillet (Pereira et al., 2024d), meteorological information for Paris (Di Antonio et al., 2023) and Rambouillet (Denjean, 2023).

#### Author contributions

DLP, AG, CG, and PF designed the research. PF, VM, CC, CD, AG, DLP, MC, GN, SC, SA, EA, AB, TB, MC, PC, LDA, SH, JH, CG, OG, BL, OL, CM, FM, BPV, RT, ST, PZ, LW, DP, SR, PMF, EP, PP, EV, AA, OF, RAP, JFD participated in sample collection and/or instruments deployment in the field. DLP, CG, GN, and AZ conducted the filter analysis. DLP, CG, AZ, AG, and PF analyzed the data. DLP drafted the initial manuscript. CG, AZ, AG, PF, PP, EP, JFD and EV reviewed and corrected the manuscript. CG and AZ provided the expertise on the HRMS analysis. CC and VC are the principal investigators of the ACROSS project. All authors made contributions to this work and approved the final version of the manuscript.

#### Competing interests

C. Cantrell is co-organizer of the special issue “Atmospheric Chemistry of the Suburban Forest – multiplatform observational campaign of the chemistry and physics of mixed urban and biogenic emissions (ACP/AMT inter-journal SI)”. The remaining authors declare no competing interests.

655 **Disclaimer.**

Publisher’s note: Copernicus Publications remains neutral with regard to jurisdictional claims made in the text, published maps, institutional affiliations, or any other geographical representation in this paper. While Copernicus Publications makes every effort to include appropriate place names, the final responsibility lies with the authors.

**Special issue statement.**

660 This article is part of the special issue “Atmospheric Chemistry of the Suburban Forest – multiplatform observational campaign of the chemistry and physics of mixed urban and biogenic emissions”. It is not associated with a conference.

**Acknowledgements.**

The ACROSS and the PEGASUS databases and their access are maintained by the French national center for atmospheric data and services AERIS as part of the DataTerra French research infrastructure. ~~DHA-80 was provided by INERIS (Institut national de l’environnement industriel et des risques) with the support of A. Albinet, O. Favez and R. Aujey Plouzeau.~~ The authors acknowledge the help of M. des Forges and M. Cayet. during the filter preparation.

**Financial support.**

The ACROSS project has received funding from the French National Research Agency (ANR) under the investment program ANR-17-MPGA-0002, and it was supported by the French National program LEFE of CNRS-INSU. This work was additionally supported by the project TRAC-AOS-A within the LEFE-CHAT national program from CNRS-INSU and from ADEME. CNRS-INSU provides support to the PEGASUS platform as a national facility. HRMS analyses were supported by a BP Next Generation fellowship awarded by the Yusuf Hamied Department of Chemistry at the University of Cambridge to CG. The PhD scholarship of DLP is supported by the IDEX program of the Université Paris Cité. AA, OF and RA (Ineris) acknowledge the French Ministry of Environment for financial support through activities of the national reference laboratory for air quality monitoring (LCSQA), as well as internal co-funding.

**References**

Akinyoola, J. A., Oluleye, A., and Gbode, I. E.: A Review of Atmospheric Aerosol Impacts on Regional Extreme Weather and Climate Events, *Aerosol Sci. Eng.*, 8, 249–274, <https://doi.org/10.1007/s41810-024-00223-x>, 2024.

Amarandei, C., Olariu, R. I., and Arsene, C.: First insights into the molecular characteristics of atmospheric organic aerosols from Iasi, Romania: Behavior of biogenic versus anthropogenic contributions and potential implications, *Sci. Total Environ.*, 877, 162830, <https://doi.org/10.1016/j.scitotenv.2023.162830>, 2023.

685 Andersen, S. T., McGillen, M. R., Xue, C., Seubert, T., Dewald, P., Türk, G. N. T. E., Schuladen, J., Denjean, C., Etienne, J.-C., Garrouste, O., Jamar, M., Harb, S., Cirtog, M., Michoud, V., Cazaunau, M., Bergé, A., Cantrell, C., Dusanter, S., Picquet-Varrault, B., Kukui, A., Mellouki, A., Carpenter, L. J., Lelieveld, J., and Crowley, J. N.: Measurement report: Sources, sinks and lifetime of NO<sub>x</sub> in a sub-urban temperate forest at night, <https://doi.org/10.5194/egusphere-2023-2848>, 24 January 2024.

Andreae, M. O. and Rosenfeld, D.: Aerosol–cloud–precipitation interactions. Part 1. The nature and sources of cloud-active aerosols, *Earth-Sci. Rev.*, 89, 13–41, <https://doi.org/10.1016/j.earscirev.2008.03.001>, 2008.

690 Artaxo, P., Machado, L., Manzi, A. O., Souza, R. A. F., Schumacher, C., Wang, J., Biscaro, T., Brito, J., Calheiros, A., Jardine, K., Medeiros, A., Portela, B., De Sá, S. S., Adachi, K., Aiken, A. C., Albrecht, R., Alexander, L., Andreae, M. O., Barbosa, H. M. J., Buseck, P., Chand, D., Comstock, J. M., Day, D. A., Dubey, M., Fan, J., Fast, J., Fisch, G., Fortner, E., Giangrande, S., Gilles, M., Goldstein, A. H., Guenther, A., Hubbe, J., Jensen, M., Jimenez, J. L., Keutsch, F. N., Kim, S., Kuang, C., Laskin, A., McKinney, K., Mei, F., Miller, M., Nascimento, R., Pauliquevis, T., Pekour, M., Peres, J., Petäjä, T., Pöhlker, C., Pöschl, U., Rizzo, L., Schmid, B., Shilling, J. E., Dias, M. A. S., Smith, J. N., Tomlinson, J. M., Tóta, J., and Wendisch, M.: The Green Ocean Amazon Experiment (GoAmazon2014/5) Observes Pollution Affecting Gases, Aerosols, Clouds, and Rainfall over the Rain Forest, *Bull. Am. Meteorol. Soc.*, 98, 981–997, <https://doi.org/10.1175/BAMS-D-15-00221.1>, 2017.

695 Atkinson, R.: Rate constants for the atmospheric reactions of alkoxy radicals: An updated estimation method, *Atmos. Environ.*, 41, 8468–8485, <https://doi.org/10.1016/j.atmosenv.2007.07.002>, 2007.

Atkinson, R. and Arey, J.: Atmospheric Degradation of Volatile Organic Compounds, *Chem. Rev.*, 103, 4605–4638, <https://doi.org/10.1021/cr0206420>, 2003.

700 Beekmann, M., Prévôt, A. S. H., Drewnick, F., Sciare, J., Pandis, S. N., Denier van der Gon, H. A. C., Crippa, M., Freutel, F., Poulain, L., Gherzi, V., Rodriguez, E., Beirle, S., Zotter, P., von der Weiden-Reinmüller, S.-L., Bressi, M., Fountoukis, C., Petetin, H., Szidat, S., Schneider, J., Rosso, A., El Haddad, I., Megaritis, A., Zhang, Q. J., Michoud, V., Slowik, J. G., Moukhtar, S., Kolmonen, P., Stohl, A., Eckhardt, S., Borbon, A., Gros, V., Marchand, N., Jaffrezo, J. L., Schwarzenboeck, A., Colomb, A., Wiedensohler, A., Borrmann, S., Lawrence, M., Baklanov, A., and Baltensperger, U.: In situ, satellite measurement and model evidence on the dominant regional contribution to fine particulate matter levels in the Paris megacity, *Atmospheric Chem. Phys.*, 15, 9577–9591, <https://doi.org/10.5194/acp-15-9577-2015>, 2015.

705 Bourtsoukidis, E., Pozzer, A., Williams, J., Makowski, D., Peñuelas, J., Matthaios, V. N., Lazoglou, G., Yañez-Serrano, A. M., Lelieveld, J., Ciais, P., Vrekoussis, M., Daskalakis, N., and Sciare, J.: High temperature sensitivity of monoterpene emissions from global vegetation, *Commun. Earth Environ.*, 5, 23, <https://doi.org/10.1038/s43247-023-01175-9>, 2024.

710 Bressi, M., Sciare, J., Gherzi, V., Bonnaire, N., Nicolas, J. B., Petit, J.-E., Moukhtar, S., Rosso, A., Mihalopoulos, N., and Féron, A.: A one-year comprehensive chemical characterisation of fine aerosol (PM<sub>2.5</sub>) at urban, suburban and rural background sites in the region of Paris (France), *Atmospheric Chem. Phys.*, 13, 7825–7844, <https://doi.org/10.5194/acp-13-7825-2013>, 2013.

715 Bressi, M., Sciare, J., Gherzi, V., Mihalopoulos, N., Petit, J.-E., Nicolas, J. B., Moukhtar, S., Rosso, A., Féron, A., Bonnaire, N., Poulakis, E., and Theodosi, C.: Sources and geographical origins of fine aerosols in Paris (France), *Atmospheric Chem. Phys.*, 14, 8813–8839, <https://doi.org/10.5194/acp-14-8813-2014>, 2014.

720 Bryant, D. J., Nelson, B. S., Swift, S. J., Budisulistiorini, S. H., Drysdale, W. S., Vaughan, A. R., Newland, M. J., Hopkins, J. R., Cash, J. M., Langford, B., Nemitz, E., Acton, W. J. F., Hewitt, C. N., Mandal, T., Gurjar, B. R., Shivani, Gadi, R., Lee, J. D., Rickard, A. R., and Hamilton, J. F.: Biogenic and anthropogenic sources of isoprene and monoterpenes and their secondary organic aerosol in Delhi, India, *Atmospheric Chem. Phys.*, 23, 61–83, <https://doi.org/10.5194/acp-23-61-2023>, 2023.

- Cahill, T. M., Seaman, V. Y., Charles, M. J., Holzinger, R., and Goldstein, A. H.: Secondary organic aerosols formed from oxidation of biogenic volatile organic compounds in the Sierra Nevada Mountains of California, *J. Geophys. Res. Atmospheres*, 111, 2006JD007178, <https://doi.org/10.1029/2006JD007178>, 2006.
- 725 Cantrell, C. and Michoud, V.: An Experiment to Study Atmospheric Oxidation Chemistry and Physics of Mixed Anthropogenic–Biogenic Air Masses in the Greater Paris Area, *Am. Meteorol. Soc.*, 599–603, <https://doi.org/10.1175/BAMS-D-21-0115.1>, 2022.
- Cao, J. J., Wu, F., Chow, J. C., Lee, S. C., Li, Y., Chen, S. W., An, Z. S., Fung, K. K., Watson, J. G., Zhu, C. S., and Liu, S. X.: Characterization and source apportionment of atmospheric organic and elemental carbon during fall and winter of 2003 in Xi'an, China, *Atmospheric Chem. Phys.*, 5, 3127–3137, <https://doi.org/10.5194/acp-5-3127-2005>, 2005.
- 730 Cavalli, F., Viana, M., Yttri, K. E., Genberg, J., and Putaud, J. P.: Toward a standardised thermal-optical protocol for measuring atmospheric organic and elemental carbon: the EUSAAR protocol, *Atmospheric Meas. Tech.*, 3, 79–89, <https://doi.org/10.5194/amt-3-79-2010>, 2010.
- Chen, B. and Kan, H.: Air pollution and population health: a global challenge, *Environ. Health Prev. Med.*, 13, 94–101, <https://doi.org/10.1007/s12199-007-0018-5>, 2008.
- 735 Chen, G., Canonaco, F., Tobler, A., Aas, W., Alastuey, A., Allan, J., Atabakhsh, S., Aurela, M., Baltensperger, U., Bougiatioti, A., De Brito, J. F., Ceburnis, D., Chazeau, B., Chebaicheb, H., Daellenbach, K. R., Ehn, M., El Haddad, I., Eleftheriadis, K., Favez, O., Flentje, H., Font, A., Fossum, K., Freney, E., Gini, M., Green, D. C., Heikkinen, L., Herrmann, H., Kalogridis, A.-C., Keernik, H., Lhotka, R., Lin, C., Lunder, C., Maasikmets, M., Manousakas, M. I., Marchand, N., Marin, C., Marmureanu, L., Mihalopoulos, N., Močnik, G., Nečki, J., O'Dowd, C., Ovadnevaite, J., Peter, T., Petit, J.-E., Pikridas, M., Matthew Platt, S., Pokorná, P., Poulain, L., Priestman, M., Riffault, V., Rinaldi, M., Róžański, K., Schwarz, J., Sciare, J., Simon, L., Skiba, A., Slowik, J. G., Sosedova, Y., Stavroulas, I., Styszko, K., Teinmaa, E., Timonen, H., Tremper, A., Vasilescu, J., Via, M., Vodička, P., Wiedensohler, A., Zografou, O., Cruz Minguillón, M., and Prévôt, A. S. H.: European aerosol phenomenology – 8: Harmonised source apportionment of organic aerosol using 22 Year-long ACSM/AMS datasets, *Environ. Int.*, 166, 107325, <https://doi.org/10.1016/j.envint.2022.107325>, 2022.
- 740 745 Cheng, Z., Luo, L., Wang, S., Wang, Y., Sharma, S., Shimadera, H., Wang, X., Bressi, M., De Miranda, R. M., Jiang, J., Zhou, W., Fajardo, O., Yan, N., and Hao, J.: Status and characteristics of ambient PM<sub>2.5</sub> pollution in global megacities, *Environ. Int.*, 89–90, 212–221, <https://doi.org/10.1016/j.envint.2016.02.003>, 2016.
- Claeys, M., Szmigielski, R., Kourtchev, I., Van Der Veken, P., Vermeylen, R., Maenhaut, W., Jaoui, M., Kleindienst, T. E., Lewandowski, M., Offenberg, J. H., and Edney, E. O.: Hydroxydicarboxylic Acids: Markers for Secondary Organic Aerosol from the Photooxidation of  $\alpha$ -Pinene, *Environ. Sci. Technol.*, 41, 1628–1634, <https://doi.org/10.1021/es0620181>, 2007.
- 750 Daellenbach, K. R., Kourtchev, I., Vogel, A. L., Bruns, E. A., Jiang, J., Petäjä, T., Jaffrezo, J.-L., Aksoyoglu, S., Kalberer, M., Baltensperger, U., El Haddad, I., and Prévôt, A. S. H.: Impact of anthropogenic and biogenic sources on the seasonal variation in the molecular composition of urban organic aerosols: a field and laboratory study using ultra-high-resolution mass spectrometry, *Atmospheric Chem. Phys.*, 19, 5973–5991, <https://doi.org/10.5194/acp-19-5973-2019>, 2019.
- 755 Denjean, C.: ACROSS\_CNRM\_RambForest\_MTO-IMIN\_L2, Aeris [dataset], <https://doi.org/10.25326/437>, 2023.
- Di Antonio, L., Di Biagio, C., Gratien, A., Hawkins, L. N., Bergé, A., and Riley, S.: ACROSS\_LISA\_PRG\_METEO\_1-Min\_L2, Aeris [dataset], <https://doi.org/10.25326/573>, 2023.

760 Ding, X., Wang, X., Gao, B., Fu, X., He, Q., Zhao, X., Yu, J., and Zheng, M.: Tracer-based estimation of secondary organic carbon in the Pearl River Delta, south China, *J. Geophys. Res. Atmospheres*, 117, 2011JD016596, <https://doi.org/10.1029/2011JD016596>, 2012.

Favez, O., Cachier, H., Sciare, J., Sarda-Estève, R., and Martinon, L.: Evidence for a significant contribution of wood burning aerosols to PM<sub>2.5</sub> during the winter season in Paris, France, *Atmos. Environ.*, 43, 3640–3644, <https://doi.org/10.1016/j.atmosenv.2009.04.035>, 2009.

765 Giorio, C., Moyroud, E., Glover, B. J., Skelton, P. C., and Kalberer, M.: Direct Surface Analysis Coupled to High-Resolution Mass Spectrometry Reveals Heterogeneous Composition of the Cuticle of *Hibiscus trionum* Petals, *Anal. Chem.*, 87, 9900–9907, <https://doi.org/10.1021/acs.analchem.5b02498>, 2015.

Giorio, C., Bortolini, C., Kourtchev, I., Tapparo, A., Bogialli, S., and Kalberer, M.: Direct target and non-target analysis of urban aerosol sample extracts using atmospheric pressure photoionisation high-resolution mass spectrometry, *Chemosphere*, 224, 786–795, <https://doi.org/10.1016/j.chemosphere.2019.02.151>, 2019.

770 Giorio, C., Doussin, J., D’Anna, B., Mas, S., Filippi, D., Denjean, C., Mallet, M. D., Bourrianne, T., Burnet, F., Cazaunau, M., Chikwililwa, C., Desboeufs, K., Feron, A., Michoud, V., Namwoonde, A., Andreae, M. O., Piketh, S. J., and Formenti, P.: Butene Emissions From Coastal Ecosystems May Contribute to New Particle Formation, *Geophys. Res. Lett.*, 49, e2022GL098770, <https://doi.org/10.1029/2022GL098770>, 2022.

775 Gros, V., Sciare, J., and Yu, T.: Air-quality measurements in megacities: Focus on gaseous organic and particulate pollutants and comparison between two contrasted cities, Paris and Beijing, *Comptes Rendus Géoscience*, 339, 764–774, <https://doi.org/10.1016/j.crte.2007.08.007>, 2007.

780 Haefelin, M., Barthès, L., Bock, O., Boitel, C., Bony, S., Bouniol, D., Chepfer, H., Chiriaco, M., Cuesta, J., Delanoë, J., Drobinski, P., Dufresne, J.-L., Flamant, C., Grall, M., Hodzic, A., Hourdin, F., Lapouge, F., Lemaître, Y., Mathieu, A., Morille, Y., Naud, C., Noël, V., O’Hirok, W., Pelon, J., Pietras, C., Protat, A., Romand, B., Scialom, G., and Vautard, R.: SIRTa, a ground-based atmospheric observatory for cloud and aerosol research, *Ann. Geophys.*, 23, 253–275, <https://doi.org/10.5194/angeo-23-253-2005>, 2005.

785 Hallquist, M., Wenger, J. C., Baltensperger, U., Rudich, Y., Simpson, D., Claeys, M., Dommen, J., Donahue, N. M., George, C., Goldstein, A. H., Hamilton, J. F., Herrmann, H., Hoffmann, T., Iinuma, Y., Jang, M., Jenkin, M. E., Jimenez, J. L., Kiendler-Scharr, A., Maenhaut, W., McFiggans, G., Mentel, Th. F., Monod, A., Prévôt, A. S. H., Seinfeld, J. H., Surratt, J. D., Szmigielski, R., and Wildt, J.: The formation, properties and impact of secondary organic aerosol: current and emerging issues, *Atmospheric Chem. Phys.*, 9, 5155–5236, <https://doi.org/10.5194/acp-9-5155-2009>, 2009.

Haywood, J.: Atmospheric Aerosols and Their Role in Climate Change, in: *Climate Change*, Elsevier, 449–463, <https://doi.org/10.1016/B978-0-444-63524-2.00027-0>, 2016.

790 He, Q., Tomaz, S., Li, C., Zhu, M., Meidan, D., Riva, M., Laskin, A., Brown, S. S., George, C., Wang, X., and Rudich, Y.: Optical Properties of Secondary Organic Aerosol Produced by Nitrate Radical Oxidation of Biogenic Volatile Organic Compounds, *Environ. Sci. Technol.*, 55, 2878–2889, <https://doi.org/10.1021/acs.est.0c06838>, 2021.

Hodzic, A., Vautard, R., Chazette, P., Menut, L., and Bessagnet, B.: Aerosol chemical and optical properties over the Paris area within ESQUIF project, *Atmospheric Chem. Phys.*, 6, 3257–3280, <https://doi.org/10.5194/acp-6-3257-2006>, 2006.

795 Iinuma, Y., Böge, O., Gräfe, R., and Herrmann, H.: Methyl-Nitrocatechols: Atmospheric Tracer Compounds for Biomass Burning Secondary Organic Aerosols, *Environ. Sci. Technol.*, 44, 8453–8459, <https://doi.org/10.1021/es102938a>, 2010.

Ion, A. C., Vermeylen, R., Kourtchev, I., Cafmeyer, J., Chi, X., Gelencsér, A., Maenhaut, W., and Claeys, M.: Polar organic compounds in rural PM<sub>2.5</sub> aerosols from K-pusztá, Hungary, during a 2003 summer field campaign: Sources and diel variations, *Atmospheric Chem. Phys.*, 5, 1805–1814, <https://doi.org/10.5194/acp-5-1805-2005>, 2005.

IPCC: Climate Change 2021 – The Physical Science Basis: Working Group I Contribution to the Sixth Assessment Report of the Intergovernmental Panel on Climate Change, 1st ed., Cambridge University Press, <https://doi.org/10.1017/9781009157896>, 2023.

Bilan démographique 2022 de l'Île-de-France : deux naissances pour un décès: <https://www.insee.fr/fr/statistiques/6968304#:~:text=La%20population%20francilienne%20augmente%20uniquement,exc%C3%A9dent%20naturel%20s'amenuise.>, last access: 29 January 2024.

Kalberer, M.: AEROSOLS | Aerosol Physics and Chemistry, in: *Encyclopedia of Atmospheric Sciences*, Elsevier, 23–31, <https://doi.org/10.1016/B978-0-12-382225-3.00049-9>, 2015.

Kanakidou, M., Seinfeld, J. H., Pandis, S. N., Barnes, I., Dentener, F. J., Facchini, M. C., Van Dingenen, R., Ervens, B., Nenes, A., Nielsen, C. J., Swietlicki, E., Putaud, J. P., Balkanski, Y., Fuzzi, S., Horth, J., Moortgat, G. K., Winterhalter, R., Myhre, C. E. L., Tsigaridis, K., Vignati, E., Stephanou, E. G., and Wilson, J.: Organic aerosol and global climate modelling: a review, *Atmospheric Chem. Phys.*, 5, 1053–1123, <https://doi.org/10.5194/acp-5-1053-2005>, 2005.

Karagulian, F., Belis, C. A., Dora, C. F. C., Prüss-Ustün, A. M., Bonjour, S., Adair-Rohani, H., and Amann, M.: Contributions to cities' ambient particulate matter (PM): A systematic review of local source contributions at global level, *Atmos. Environ.*, 120, 475–483, <https://doi.org/10.1016/j.atmosenv.2015.08.087>, 2015.

Karanasiou, A., Panteliadis, P., Perez, N., Minguillón, M. C., Pandolfi, M., Titos, G., Viana, M., Moreno, T., Querol, X., and Alastuey, A.: Evaluation of the Semi-Continuous OCEC analyzer performance with the EUSAAR2 protocol, *Sci. Total Environ.*, 747, 141266, <https://doi.org/10.1016/j.scitotenv.2020.141266>, 2020.

Kim, S., Kramer, R. W., and Hatcher, P. G.: Graphical Method for Analysis of Ultrahigh-Resolution Broadband Mass Spectra of Natural Organic Matter, the Van Krevelen Diagram, *Anal. Chem.*, 75, 5336–5344, <https://doi.org/10.1021/ac034415p>, 2003.

Kourtchev, I., Copolovici, L., Claeys, M., and Maenhaut, W.: Characterization of Atmospheric Aerosols at a Forested Site in Central Europe, *Environ. Sci. Technol.*, 43, 4665–4671, <https://doi.org/10.1021/es803055w>, 2009.

Kourtchev, I., Fuller, S., Aalto, J., Ruuskanen, T. M., McLeod, M. W., Maenhaut, W., Jones, R., Kulmala, M., and Kalberer, M.: Molecular Composition of Boreal Forest Aerosol from Hyytiälä, Finland, Using Ultrahigh Resolution Mass Spectrometry, *Environ. Sci. Technol.*, 47, 4069–4079, <https://doi.org/10.1021/es3051636>, 2013.

Kourtchev, I., O'Connor, I. P., Giorio, C., Fuller, S. J., Kristensen, K., Maenhaut, W., Wenger, J. C., Sodeau, J. R., Glasius, M., and Kalberer, M.: Effects of anthropogenic emissions on the molecular composition of urban organic aerosols: An ultrahigh resolution mass spectrometry study, *Atmos. Environ.*, 89, 525–532, <https://doi.org/10.1016/j.atmosenv.2014.02.051>, 2014.

Kourtchev, I., Doussin, J.-F., Giorio, C., Mahon, B., Wilson, E. M., Maurin, N., Pangui, E., Venables, D. S., Wenger, J. C., and Kalberer, M.: Molecular composition of fresh and aged secondary organic aerosol from a mixture of biogenic volatile compounds: a high-resolution mass spectrometry study, *Atmospheric Chem. Phys.*, 15, 5683–5695, <https://doi.org/10.5194/acp-15-5683-2015>, 2015.

Kourtchev, I., Godoi, R. H. M., Connors, S., Levine, J. G., Archibald, A. T., Godoi, A. F. L., Paralovo, S. L., Barbosa, C. G. G., Souza, R. A. F., Manzi, A. O., Seco, R., Sjöstedt, S., Park, J.-H., Guenther, A., Kim, S., Smith, J., Martin, S. T., and

- Kalberer, M.: Molecular composition of organic aerosols in central Amazonia: an ultra-high-resolution mass spectrometry study, *Atmospheric Chem. Phys.*, 16, 11899–11913, <https://doi.org/10.5194/acp-16-11899-2016>, 2016.
- 835 Kristensen, K., Enggrob, K. L., King, S. M., Worton, D. R., Platt, S. M., Mortensen, R., Rosenoern, T., Surratt, J. D., Bilde, M., Goldstein, A. H., and Glasius, M.: Formation and occurrence of dimer esters of pinene oxidation products in atmospheric aerosols, *Atmospheric Chem. Phys.*, 13, 3763–3776, <https://doi.org/10.5194/acp-13-3763-2013>, 2013.
- 840 Kristensen, K., Cui, T., Zhang, H., Gold, A., Glasius, M., and Surratt, J. D.: Dimers in  $\alpha$ -pinene secondary organic aerosol: effect of hydroxyl radical, ozone, relative humidity and aerosol acidity, *Atmospheric Chem. Phys.*, 14, 4201–4218, <https://doi.org/10.5194/acp-14-4201-2014>, 2014.
- Kroll, J. H. and Seinfeld, J. H.: Chemistry of secondary organic aerosol: Formation and evolution of low-volatility organics in the atmosphere, *Atmos. Environ.*, 42, 3593–3624, <https://doi.org/10.1016/j.atmosenv.2008.01.003>, 2008.
- 845 Lanzafame, G. M., Srivastava, D., Favez, O., Bandowe, B. A. M., Shahpoury, P., Lammel, G., Bonnaire, N., Alleman, L. Y., Couvidat, F., Bessagnet, B., and Albinet, A.: One-year measurements of secondary organic aerosol (SOA) markers in the Paris region (France): Concentrations, gas/particle partitioning and SOA source apportionment, *Sci. Total Environ.*, 757, 143921, <https://doi.org/10.1016/j.scitotenv.2020.143921>, 2021.
- Li, Y., Li, J., Zhao, Y., Lei, M., Zhao, Y., Jian, B., Zhang, M., and Huang, J.: Long-term variation of boundary layer height and possible contribution factors: A global analysis, *Sci. Total Environ.*, 796, 148950, <https://doi.org/10.1016/j.scitotenv.2021.148950>, 2021.
- 850 Lin, P., Hu, M., Deng, Z., Slanina, J., Han, S., Kondo, Y., Takegawa, N., Miyazaki, Y., Zhao, Y., and Sugimoto, N.: Seasonal and diurnal variations of organic carbon in PM<sub>2.5</sub> in Beijing and the estimation of secondary organic carbon, *J. Geophys. Res. Atmospheres*, 114, 2008JD010902, <https://doi.org/10.1029/2008JD010902>, 2009.
- 855 Lin, P., Rincon, A. G., Kalberer, M., and Yu, J. Z.: Elemental Composition of HULIS in the Pearl River Delta Region, China: Results Inferred from Positive and Negative Electrospray High Resolution Mass Spectrometric Data, *Environ. Sci. Technol.*, 46, 7454–7462, <https://doi.org/10.1021/es300285d>, 2012.
- Luo, H., Chen, J., Li, G., and An, T.: Formation kinetics and mechanism of ozone and secondary organicaerosols from photochemical oxidation of different aromatic hydrocarbons: dependence of NO<sub>x</sub> and organic substituent, <https://doi.org/10.5194/acp-2021-29>, 25 January 2021.
- 860 Ma, J., Li, X., Gu, P., Dallmann, T. R., Presto, A. A., and Donahue, N. M.: Estimating ambient particulate organic carbon concentrations and partitioning using thermal optical measurements and the volatility basis set, *Aerosol Sci. Technol.*, 50, 638–651, <https://doi.org/10.1080/02786826.2016.1158778>, 2016.
- 865 Maison, A., Lugon, L., Park, S.-J., Baudic, A., Cantrell, C., Couvidat, F., D’Anna, B., Di Biagio, C., Gratien, A., Gros, V., Kalalian, C., Kammer, J., Michoud, V., Petit, J.-E., Shahin, M., Simon, L., Valari, M., Vigneron, J., Tuzet, A., and Sartelet, K.: Significant impact of urban tree biogenic emissions on air quality estimated by a bottom-up inventory and chemistry transport modeling, *Atmospheric Chem. Phys.*, 24, 6011–6046, <https://doi.org/10.5194/acp-24-6011-2024>, 2024.
- Malik, T. G., Sahu, L. K., Gupta, M., Mir, B. A., Gajbhiye, T., Dubey, R., Clavijo McCormick, A., and Pandey, S. K.: Environmental Factors Affecting Monoterpene Emissions from Terrestrial Vegetation, *Plants*, 12, 3146, <https://doi.org/10.3390/plants12173146>, 2023.
- MathWorks Inc: MATLAB version: 9.13.0 (R2022b), 2022.



- 870 McFiggans, G., Mentel, T. F., Wildt, J., Pullinen, I., Kang, S., Kleist, E., Schmitt, S., Springer, M., Tillmann, R., Wu, C., Zhao, D., Hallquist, M., Faxon, C., Le Breton, M., Hallquist, A. M., Simpson, D., Bergström, R., Jenkin, M. E., Ehn, M., Thornton, J. A., Alfarra, M. R., Bannan, T. J., Percival, C. J., Priestley, M., Topping, D., and Kiendler-Scharr, A.: Secondary organic aerosol reduced by mixture of atmospheric vapours, *Nature*, 565, 587–593, <https://doi.org/10.1038/s41586-018-0871-y>, 2019.
- 875 Menut, L., Cholakian, A., Siour, G., Lapere, R., Pennel, R., Mailler, S., and Bessagnet, B.: Impact of Landes forest fires on air quality in France during the 2022 summer, *Atmospheric Chem. Phys.*, 23, 7281–7296, <https://doi.org/10.5194/acp-23-7281-2023>, 2023.
- Michoud, V., Hallemans, E., Chiappini, L., Leoz-Garziandia, E., Colomb, A., Dusanter, S., Fronval, I., Gheusi, F., Jaffrezo, J.-L., Léonardis, T., Locoge, N., Marchand, N., Sauvage, S., Sciare, J., and Doussin, J.-F.: Molecular characterization of gaseous and particulate oxygenated compounds at a remote site in Cape Corsica in the western Mediterranean Basin, *Atmospheric Chem. Phys.*, 21, 8067–8088, <https://doi.org/10.5194/acp-21-8067-2021>, 2021.
- 880 Molina, L. T., Madronich, S., Gaffney, J. S., Apel, E., De Foy, B., Fast, J., Ferrare, R., Herndon, S., Jimenez, J. L., Lamb, B., Osornio-Vargas, A. R., Russell, P., Schauer, J. J., Stevens, P. S., Volkamer, R., and Zavala, M.: An overview of the MILAGRO 2006 Campaign: Mexico City emissions and their transport and transformation, *Atmospheric Chem. Phys.*, 10, 8697–8760, <https://doi.org/10.5194/acp-10-8697-2010>, 2010.
- 885 Office National des Forêts: Forêt domaniale de Rambouillet, Vivre For., 2023.
- Pereira, D., Gratien, A., Formenti, P., Giorio, C., Chevaillier, S., and Noyalet, G.: ACROSS\_LISA\_PRG\_OC-EC\_L2, Aeris [dataset], <https://doi.org/10.25326/682>, 2024a.
- Pereira, D., Gratien, A., Giorio, C., and Formenti, P.: ACROSS\_LISA\_PRG\_Orbitrap\_L2, Aeris [dataset], <https://doi.org/10.25326/683>, 2024b.
- 890 Pereira, D., Gratien, A., Formenti, P., Giorio, C., Chevaillier, S., and Noyalet, G.: ACROSS\_LISA\_RambForest\_OC-EC\_L2, Aeris [dataset], <https://doi.org/10.25326/681>, 2024c.
- Pereira, D., Gratien, A., Giorio, C., and Formenti, P.: ACROSS\_LISA\_RambForest\_Orbitrap\_L2, Aeris [dataset], <https://doi.org/10.25326/684>, 2024d.
- 895 Rattanavaraha, W., Chu, K., Budisulistiorini, S. H., Riva, M., Lin, Y.-H., Edgerton, E. S., Baumann, K., Shaw, S. L., Guo, H., King, L., Weber, R. J., Neff, M. E., Stone, E. A., Offenberg, J. H., Zhang, Z., Gold, A., and Surratt, J. D.: Assessing the impact of anthropogenic pollution on isoprene-derived secondary organic aerosol formation in PM<sub>2.5</sub>; collected from the Birmingham, Alabama, ground site during the 2013 Southern Oxidant and Aerosol Study, *Atmospheric Chem. Phys.*, 16, 4897–4914, <https://doi.org/10.5194/acp-16-4897-2016>, 2016.
- 900 Rosenfeld, D., Sherwood, S., Wood, R., and Donner, L.: Climate Effects of Aerosol-Cloud Interactions, *Science*, 343, 379–380, <https://doi.org/10.1126/science.1247490>, 2014.
- Sato, K., Hatakeyama, S., and Imamura, T.: Secondary Organic Aerosol Formation during the Photooxidation of Toluene: NO<sub>x</sub> Dependence of Chemical Composition, *J. Phys. Chem. A*, 111, 9796–9808, <https://doi.org/10.1021/jp071419f>, 2007.
- 905 Sato, K., Ikemori, F., Ramasamy, S., Iijima, A., Kumagai, K., Fushimi, A., Fujitani, Y., Chatani, S., Tanabe, K., Takami, A., Tago, H., Saito, Y., Saito, S., Hoshi, J., and Morino, Y.: Formation of secondary organic aerosol tracers from anthropogenic and biogenic volatile organic compounds under varied NO and oxidant conditions, *Atmospheric Environ. X*, 14, 100169, <https://doi.org/10.1016/j.aeaoa.2022.100169>, 2022.

Mis en forme : Français (France)

Sciare, J., d'Argouges, O., Zhang, Q. J., Sarda-Estève, R., Gaimoz, C., Gros, V., Beekmann, M., and Sanchez, O.: Comparison between simulated and observed chemical composition of fine aerosols in Paris (France) during springtime: contribution of regional versus continental emissions, *Atmospheric Chem. Phys.*, 10, 11987–12004, <https://doi.org/10.5194/acp-10-11987-2010>, 2010.

910 Sheehan, P. E. and Bowman, F. M.: Estimated Effects of Temperature on Secondary Organic Aerosol Concentrations, *Environ. Sci. Technol.*, 35, 2129–2135, <https://doi.org/10.1021/es001547g>, 2001.

Shen, R.-Q., Ding, X., He, Q.-F., Cong, Z.-Y., Yu, Q.-Q., and Wang, X.-M.: Seasonal variation of secondary organic aerosol tracers in Central Tibetan Plateau, *Atmospheric Chem. Phys.*, 15, 8781–8793, <https://doi.org/10.5194/acp-15-8781-2015>, 2015.

915 Shrivastava, M., Andreae, M. O., Artaxo, P., Barbosa, H. M. J., Berg, L. K., Brito, J., Ching, J., Easter, R. C., Fan, J., Fast, J. D., Feng, Z., Fuentes, J. D., Glasius, M., Goldstein, A. H., Alves, E. G., Gomes, H., Gu, D., Guenther, A., Jathar, S. H., Kim, S., Liu, Y., Lou, S., Martin, S. T., McNeill, V. F., Medeiros, A., De Sá, S. S., Shilling, J. E., Springston, S. R., Souza, R. A. F., Thornton, J. A., Isaacman-VanWertz, G., Yee, L. D., Ynoue, R., Zaveri, R. A., Zelenyuk, A., and Zhao, C.: Urban pollution greatly enhances formation of natural aerosols over the Amazon rainforest, *Nat. Commun.*, 10, 1046, <https://doi.org/10.1038/s41467-019-08909-4>, 2019.

920 Srivastava, D., Favez, O., Bonnaire, N., Lucarelli, F., Haeffelin, M., Perraudin, E., Gros, V., Villenave, E., and Albinet, A.: Speciation of organic fractions does matter for aerosol source apportionment. Part 2: Intensive short-term campaign in the Paris area (France), *Sci. Total Environ.*, 634, 267–278, <https://doi.org/10.1016/j.scitotenv.2018.03.296>, 2018.

925 Srivastava, D., Favez, O., Petit, J.-E., Zhang, Y., Sofowote, U. M., Hopke, P. K., Bonnaire, N., Perraudin, E., Gros, V., Villenave, E., and Albinet, A.: Speciation of organic fractions does matter for aerosol source apportionment. Part 3: Combining off-line and on-line measurements, *Sci. Total Environ.*, 690, 944–955, <https://doi.org/10.1016/j.scitotenv.2019.06.378>, 2019.

Surratt, J. D., Kroll, J. H., Kleindienst, T. E., Edney, E. O., Claeys, M., Sorooshian, A., Ng, N. L., Offenberg, J. H., Lewandowski, M., Jaoui, M., Flagan, R. C., and Seinfeld, J. H.: Evidence for Organosulfates in Secondary Organic Aerosol, *Environ. Sci. Technol.*, 41, 517–527, <https://doi.org/10.1021/es062081q>, 2007.

930 Surratt, J. D., Gómez-González, Y., Chan, A. W. H., Vermeylen, R., Shahgholi, M., Kleindienst, T. E., Edney, E. O., Offenberg, J. H., Lewandowski, M., Jaoui, M., Maenhaut, W., Claeys, M., Flagan, R. C., and Seinfeld, J. H.: Organosulfate Formation in Biogenic Secondary Organic Aerosol, *J. Phys. Chem. A*, 112, 8345–8378, <https://doi.org/10.1021/jp802310p>, 2008.

935 Wang, K., Zhang, Y., Huang, R.-J., Cao, J., and Hoffmann, T.: UHPLC-Orbitrap mass spectrometric characterization of organic aerosol from a central European city (Mainz, Germany) and a Chinese megacity (Beijing), *Atmos. Environ.*, 189, 22–29, <https://doi.org/10.1016/j.atmosenv.2018.06.036>, 2018.

Wang, Z., Ge, Y., Bi, S., Liang, Y., and Shi, Q.: Molecular characterization of organic aerosol in winter from Beijing using UHPLC-Orbitrap MS, *Sci. Total Environ.*, 812, 151507, <https://doi.org/10.1016/j.scitotenv.2021.151507>, 2022.

940 Wang, Z., Cao, R., Li, B., Cai, M., Peng, Z.-R., Zhang, G., Lu, Q., He, H., Zhang, J., Shi, K., Liu, Y., Zhang, H., and Hu, X.: Characterizing nighttime vertical profiles of atmospheric particulate matter and ozone in a megacity of south China using unmanned aerial vehicle measurements, *Environ. Res.*, 236, 116854, <https://doi.org/10.1016/j.envres.2023.116854>, 2023.

Wozniak, A. S., Bauer, J. E., Sleighter, R. L., Dickhut, R. M., and Hatcher, P. G.: Technical Note: Molecular characterization of aerosol-derived water soluble organic carbon using ultrahigh resolution electrospray ionization Fourier transform ion

- 945 cyclotron resonance mass spectrometry, *Atmospheric Chem. Phys.*, 8, 5099–5111, <https://doi.org/10.5194/acp-8-5099-2008>, 2008.
- Xu, Z., Feng, W., Wang, Y., Ye, H., Wang, Y., Liao, H., and Xie, M.: Potential underestimation of ambient brown carbon absorption based on the methanol extraction method and its impacts on source analysis, *Atmospheric Chem. Phys.*, 22, 13739–13752, <https://doi.org/10.5194/acp-22-13739-2022>, 2022.
- 950 Yan, B., Zheng, M., Hu, Y., Ding, X., Sullivan, A. P., Weber, R. J., Baek, J., Edgerton, E. S., and Russell, A. G.: Roadside, Urban, and Rural Comparison of Primary and Secondary Organic Molecular Markers in Ambient PM<sub>2.5</sub>, *Environ. Sci. Technol.*, 43, 4287–4293, <https://doi.org/10.1021/es900316g>, 2009.
- Yasmeen, F., Vermeylen, R., Szmigielski, R., Iinuma, Y., Böge, O., Herrmann, H., Maenhaut, W., and Claeys, M.: Terpenylic acid and related compounds: precursors for dimers in secondary organic aerosol from the ozonolysis of  $\alpha$ - and  $\beta$ -pinene, *Atmospheric Chem. Phys.*, 10, 9383–9392, <https://doi.org/10.5194/acp-10-9383-2010>, 2010.
- 955 Yassine, M. M., Harir, M., Dabek-Zlotorzynska, E., and Schmitt-Kopplin, P.: Structural characterization of organic aerosol using Fourier transform ion cyclotron resonance mass spectrometry: Aromaticity equivalent approach, *Rapid Commun. Mass Spectrom.*, 28, 2445–2454, <https://doi.org/10.1002/rcm.7038>, 2014.
- Yee, L. D., Isaacman-VanWertz, G., Wernis, R. A., Kreisberg, N. M., Glasius, M., Riva, M., Surratt, J. D., De Sá, S. S., Martin, S. T., Alexander, M. L., Palm, Brett B., Hu, W., Campuzano-Jost, P., Day, D. A., Jimenez, J. L., Liu, Y., Misztal, P. K., Artaxo, P., Viegas, J., Manzi, A., De Souza, R. A. F., Edgerton, E. S., Baumann, K., and Goldstein, A. H.: Natural and Anthropogenically Influenced Isoprene Oxidation in Southeastern United States and Central Amazon, *Environ. Sci. Technol.*, 54, 5980–5991, <https://doi.org/10.1021/acs.est.0c00805>, 2020.
- 960 Yoo, H. Y., Kim, K. A., Kim, Y. P., Jung, C. H., Shin, H. J., Moon, K. J., Park, S. M., and Lee, J. Y.: Validation of SOC Estimation Using OC and EC Concentration in PM<sub>2.5</sub> Measured at Seoul, *Aerosol Air Qual. Res.*, 22, 210388, <https://doi.org/10.4209/aaqr.210388>, 2022.
- Zhang, H., Yee, L. D., Lee, B. H., Curtis, M. P., Worton, D. R., Isaacman-VanWertz, G., Offenberg, J. H., Lewandowski, M., Kleindienst, T. E., Beaver, M. R., Holder, A. L., Lonneman, W. A., Docherty, K. S., Jaoui, M., Pye, H. O. T., Hu, W., Day, D. A., Campuzano-Jost, P., Jimenez, J. L., Guo, H., Weber, R. J., De Gouw, J., Koss, A. R., Edgerton, E. S., Brune, W., Mohr, C., Lopez-Hilfiker, F. D., Lutz, A., Kreisberg, N. M., Spielman, S. R., Hering, S. V., Wilson, K. R., Thornton, J. A., and Goldstein, A. H.: Monoterpenes are the largest source of summertime organic aerosol in the southeastern United States, *Proc. Natl. Acad. Sci.*, 115, 2038–2043, <https://doi.org/10.1073/pnas.1717513115>, 2018.
- 970 Zhang, Q., Jimenez, J. L., Canagaratna, M. R., Allan, J. D., Coe, H., Ulbrich, I., Alfarra, M. R., Takami, A., Middlebrook, A. M., Sun, Y. L., Dzepina, K., Dunlea, E., Docherty, K., DeCarlo, P. F., Salcedo, D., Onasch, T., Jayne, J. T., Miyoshi, T., Shimono, A., Hatakeyama, S., Takegawa, N., Kondo, Y., Schneider, J., Drewnick, F., Borrmann, S., Weimer, S., Demerjian, K., Williams, P., Bower, K., Bahreini, R., Cottrell, L., Griffin, R. J., Rautiainen, J., Sun, J. Y., Zhang, Y. M., and Worsnop, D. R.: Ubiquity and dominance of oxygenated species in organic aerosols in anthropogenically-influenced Northern Hemisphere midlatitudes, *Geophys. Res. Lett.*, 34, 2007GL029979, <https://doi.org/10.1029/2007GL029979>, 2007.
- 975 Zhang, Q., Hu, W., Ren, H., Yang, J., Deng, J., Wang, D., Sun, Y., Wang, Z., Kawamura, K., and Fu, P.: Diurnal variations in primary and secondary organic aerosols in an eastern China coastal city: The impact of land-sea breezes, *Environ. Pollut.*, 319, 121016, <https://doi.org/10.1016/j.envpol.2023.121016>, 2023.
- Zhang, Q. J., Beekmann, M., Drewnick, F., Freutel, F., Schneider, J., Crippa, M., Prevot, A. S. H., Baltensperger, U., Poulain, L., Wiedensohler, A., Sciare, J., Gros, V., Borbon, A., Colomb, A., Michoud, V., Doussin, J.-F., Denier van der Gon, H. A. C., Haeffelin, M., Dupont, J.-C., Siour, G., Petetin, H., Bessagnet, B., Pandis, S. N., Hodzic, A., Sanchez, O., Honoré, C., and

- 985 Perrussel, O.: Formation of organic aerosol in the Paris region during the MEGAPOLI summer campaign: evaluation of the  
volatility-basis-set approach within the CHIMERE model, *Atmospheric Chem. Phys.*, 13, 5767–5790,  
<https://doi.org/10.5194/acp-13-5767-2013>, 2013.
- Zhang, Y., Sun, K., Gao, Z., Pan, Z., Shook, M. A., and Li, D.: Diurnal Climatology of Planetary Boundary Layer Height Over  
the Contiguous United States Derived From AMDAR and Reanalysis Data, *J. Geophys. Res. Atmospheres*, 125,  
990 e2020JD032803, <https://doi.org/10.1029/2020JD032803>, 2020.
- Zherebker, Z., Babcock, O., Pereira, D., D’Aronco, S., Filippi, D., Solda, L., Michoud, V., Gratien, A., Cirtog, M., Cantrell,  
C., Formenti, P., and Giorio, C.: Decreasing the uncertainty in the comparison of molecular fingerprints of organic aerosols  
with H/D exchange mass spectrometry, *Rev.*, 2024.
- Zhu, C., Kawamura, K., and Fu, P.: Seasonal variations of biogenic secondary organic aerosol tracers in Cape Hedo, Okinawa,  
995 *Atmos. Environ.*, 130, 113–119, <https://doi.org/10.1016/j.atmosenv.2015.08.069>, 2016.
- Zielinski, A. T., Kourtchev, I., Bortolini, C., Fuller, S., Giorio, C., Popoola, O. A. M., Bogialli, S., Tapparo, A., Jones, R., and  
Kalberer, M.: A new processing scheme for ultra-high resolution direct infusion mass spectrometry data, *Atmos. Environ.*,  
178, 129–139, <https://doi.org/10.1016/j.atmosenv.2018.01.034>, 2018.